

AD-A132 928

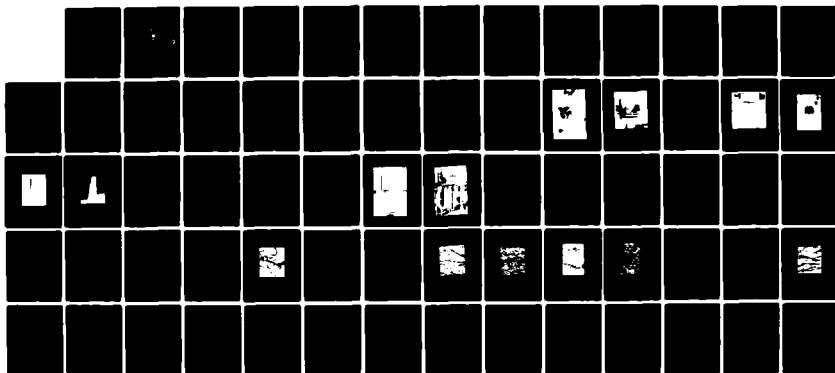
FATIGUE CRACK GROWTH RATES OF HIGH-MAGNESIUM  
ALUMINUM-MAGNESIUM ALLOYS AS..(U) NAVAL POSTGRADUATE  
SCHOOL MONTEREY CA K D OBERHOFER JUN 83

1/1

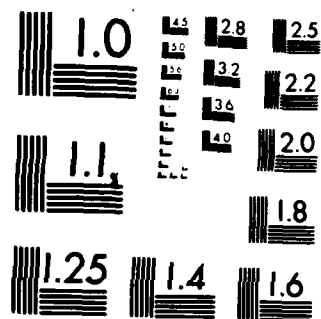
UNCLASSIFIED

F/G 11/6

NL



END  
DATE  
FILMED  
10 83  
DTIC



MICROCOPY RESOLUTION TEST CHART  
NATIONAL BUREAU OF STANDARDS 1963-A

AD A 132928

2

# NAVAL POSTGRADUATE SCHOOL

Monterey, California



DTIC  
ELECTE  
SEP 27 1983  
S A D

## THESIS

FATIGUE CRACK GROWTH RATES OF HIGH-  
MAGNESIUM ALUMINUM-MAGNESIUM ALLOYS AS  
INFLUENCED BY SOLUTION TREATMENT TIME  
AND ALLOY CONTENT

by

Kurt D. Oberhofer

June 1983

Thesis Advisor:

T.R. McNelley

Approved for public release; distribution unlimited.

DTIC FILE COPY

83 09 26 073

UNCLASSIFIED

SECURITY CLASSIFICATION OF THIS PAGE (When Data Entered)

REPORT DOCUMENTATION PAGE		READ INSTRUCTIONS BEFORE COMPLETING FORM	
1. REPORT NUMBER		2. RECIPIENT'S CATALOG NUMBER	
4. TITLE (and Subtitle) Fatigue Crack Growth Rates of High-Magnesium Aluminum-Magnesium Alloys as Influenced by Solution Treatment Time and Alloy Content		5. TYPE OF REPORT & PERIOD COVERED Master's Thesis June 1983	
7. AUTHOR(s) Kurt D. Oberhofer		6. PERFORMING ORG. REPORT NUMBER	
9. PERFORMING ORGANIZATION NAME AND ADDRESS Naval Postgraduate School Monterey, California 93940		8. CONTRACT OR GRANT NUMBER(s)	
11. CONTROLLING OFFICE NAME AND ADDRESS Naval Postgraduate School Monterey, California 93940		10. PROGRAM ELEMENT, PROJECT, TASK AREA & WORK UNIT NUMBERS	
14. MONITORING AGENCY NAME & ADDRESS (if different from Controlling Office)		12. REPORT DATE June 1983	
		13. NUMBER OF PAGES 68	
		15. SECURITY CLASS. (of this report)	
		15a. DECLASSIFICATION/DOWNGRADING SCHEDULE	
16. DISTRIBUTION STATEMENT (of this Report)  Approved for Public Release; Distribution Unlimited			
17. DISTRIBUTION STATEMENT (of the abstract entered in Block 20, if different from Report)			
18. SUPPLEMENTARY NOTES			
19. KEY WORDS (Continue on reverse side if necessary and identify by block number) High-Magnesium Aluminum-Magnesium Alloys Fatigue Crack Growth, Solution Treatment vs Stress Intensity Metal Fatigue Crack Propagation, Stress Intensity			
20. ABSTRACT (Continue on reverse side if necessary and identify by block number) <div> <div></div> <div> <p>Test equipment was fabricated and fatigue crack propagation data were obtained for aluminum alloy 7075-T6 and for thermomechanically processed Al-10.2 Wt Pct Mg-0.52 Wt Pct Mn, and Al-8.14 Wt Pct Mg-0.40 Wt Pct Cu alloys. The crack growth data and fractographic information obtained for the 7075-T6 alloy were consistent with data in the literature. The manganese containing alloy was solution treated for nine and twenty-five</p> </div> </div>			

DD FORM 1 JAN 73 1473

EDITION OF 1 NOV 65 IS OBSOLETE  
S/N 0102-LF-014-6601

UNCLASSIFIED

1

SECURITY CLASSIFICATION OF THIS PAGE (When Data Entered)

**SECURITY CLASSIFICATION OF THIS PAGE (When Data Entered)**

hour periods. Observed was a decrease in the fatigue crack growth resistance for the longer solutioning time, which appears to be due to the formation and coarsening of Mn Al<sub>6</sub> precipitates which fail to dissolve in solution treatment during thermomechanical processing. The copper containing alloy exhibited better crack growth resistance than the 7075-T6 alloy. This alloy has a more diffuse cell structure, relatively little precipitated Mg<sub>2</sub>Al<sub>3</sub>, and no constituent particles associated with cell or grain boundaries.

Accession For

DTIC  
COPY  
INSPECTED  
2

SECURITY CLASSIFICATION OF THIS PAGE (When Data Entered)

Approved for Public Release; Distribution Unlimited.

Fatigue Crack Growth Rates of High-Magnesium  
Aluminum-Magnesium Alloys as Influenced by  
Solution Treatment Time and Alloy Content

by

Kurt D. Oberhofer  
Lieutenant, United States Navy  
B.S., State University New York Maritime College, 1977

Submitted in partial fulfillment of the  
requirements for the degree of

MASTER OF SCIENCE IN MECHANICAL ENGINEERING

from the

NAVAL POSTGRADUATE SCHOOL  
June 1983

Author:

*Kurt D. Oberhofer*

Approved by:

*Larry R. McNeely*

Thesis Advisor

*J. J. Marto*

Second Reader

*J. J. Marto*

Chairman, Department of Mechanical Engineering

*John Dyer*

Dean of Science and Engineering

## ABSTRACT

Test equipment was fabricated and fatigue crack propagation data were obtained for aluminum alloy 7075-T6 and for thermomechanically processed Al-10.2 Wt Pct Mg-0.52 Wt Pct Mn, and Al-8.14 Wt Pct Mg-0.40 Wt Pct Cu alloys. The crack growth data and fractographic information obtained for the 7075-T6 alloy were consistent with data in the literature. The manganese containing alloy was solution treated for nine and twenty-five hour periods. Observed was a decrease in the fatigue crack growth resistance for the longer solutioning time, which appears to be due to the formation and coarsening of Mn Al<sub>6</sub> precipitates which fail to dissolve in solution treatment during thermomechanical processing. The copper containing alloy exhibited better crack growth resistance than the 7075-T6 alloy. This alloy has a more diffuse cell structure, relatively little precipitated Mg<sub>5</sub>Al<sub>8</sub>, and no constituent particles associated with cell or grain boundaries.

## TABLE OF CONTENTS

I.	INTRODUCTION . . . . .	12
	A. PRIMARY PURPOSE . . . . .	12
	B. BACKGROUND . . . . .	13
II.	EXPERIMENTAL PROCEDURES . . . . .	15
	A. EQUIPMENT FABRICATION . . . . .	15
	B. MATERIAL PROCESSING . . . . .	16
III.	FATIGUE CRACK GROWTH MEASUREMENT . . . . .	29
	A. MEASUREMENT TECHNIQUE . . . . .	29
	B. TENSILE TESTING . . . . .	31
	C. METALLOGRAPHY . . . . .	31
IV.	RESULTS AND DISCUSSION . . . . .	34
	A. MATERIAL PROCESSING . . . . .	34
	B. RESULTING TENSILE PROPERTIES . . . . .	34
	C. FATIGUE CRACK PROPAGATION 7075-T6 ALLOY . .	35
	1. Scanning Electron Microscopy . . . . .	35
	D. FATIGUE CRACK PROPAGATION MANGANESE	
	CONTAINING ALLOY . . . . .	36
	1. Scanning Electron Microscopy (SEM) . .	36
	2. Transmission Electron Microscopy . . .	37
	3. Optical Microscopy . . . . .	38
	E. FATIGUE CRACK PROPAGATION IN THE COPPER	
	CONTAINING ALLOY . . . . .	39
	1. Scanning Electron Microscopy . . . . .	40
	2. Optical Microscopy . . . . .	40
	3. Transmission Electron Microscopy . . .	41

V.	CONCLUSIONS AND RECOMMENDATIONS . . . . .	55
A.	CONCLUSIONS . . . . .	55
B.	RECOMMENDATIONS . . . . .	55
APPENDIX A:	FORTRAN PROGRAM FATIGUE 1 . . . . .	57
APPENDIX B:	FORTRAN PROGRAM FATIGUE 2 . . . . .	58
APPENDIX C:	FORTRAN PROGRAM RESULTS . . . . .	60
LIST OF REFERENCES	. . . . .	66
INITIAL DISTRIBUTION LIST	. . . . .	68

LIST OF TABLES

I. TABLE OF ALLOY COMPOSITIONS . . . . . 17

## LIST OF FIGURES

2.1	DIAGRAM OF CLEVIS ASSEMBLY MACHINED FROM 4140 STEEL .	20
2.2	THE ALIGNMENT APPARATUS AS MOUNTED ON THE MTS MACHINE, SHOWING THE DIAL INDICATOR AND LOAD CELL DURING CENTERING OF LOAD CELL . . . . .	21
2.3	THE ALIGNMENT BAR CLAMP AS MOUNTED ON THE LEFT HAND SIDE OF THE LOAD FRAME ASSEMBLY CONSTRUCTED OF ALUMINUM AND SUPPORTING STEEL ALIGNMENT BAR . . . . .	22
2.4	DIAGRAM SHOWING THE SECTIONING OF THE AS-CAST INGOT TO OBTAIN BILLETS FOR THERMOMECHANICAL PROCESSING . . . . .	23
2.5	A ROLLING BILLET ON THE RUN-IN TABLE OF THE ROLLING MILL . . . . .	24
2.6	AN AS-ROLLED SAMPLE OF A1-10.2 WT PCT Mg-0.52 WT PCT Mn ALLOY; THE SAMPLE WIDTH IS APPROXIMATELY THREE INCHES . . . . .	25
2.7	THE ORIGINAL DESIGN OF MACHINED SPECIMEN WITH LARGE PINHOLES AT EACH END TO FIT IN THE CLEVIS ASSEMBLY .	26
2.8	THE REDESIGN OF MACHINED SPECIMEN. THREE SMALLER HOLES WERE SUBSTITUTED FOR LARGER PINHOLES IN ORIGINAL DESIGN . . . . .	27
2.9	SCHEMATIC DIAGRAM OF FINAL DESIGN OF THE CENTER- CRACK TENSION TEST SPECIMEN USED FOR FATIGUE CRACK GROWTH MEASUREMENT . . . . .	28
3.1	SPECIMEN MOUNTED IN THE CLEVIS ASSEMBLY; CHECK FOR ALIGNMENT USES THE DIAL INDICATOR; ABOVE IS THE LOAD CELL AND BELOW IS THE HYDRAULIC RAM . . . . .	32

3.2	OPTICAL DEVICE USED TO MEASURE CRACK LENGTH, A BAUSCH & LOMB 22.7 mm, 6x TELESCOPE IN CONJUNCTION WITH A NIKON 86 mm ZOOM LENS . . . . .	33
4.1	FATIGUE CRACK PROPAGATION DATA FOR 7075-T6 ALLOY . .	42
4.2	A SCHEMATIC SHOWING SCANNING ELECTRON MICROGRAPH LOCATIONS ON THE FATIGUE CRACK SURFACE FOR THE 7075-T6 AND THE MANGANESE, AND COPPER CONTAINING ALLOYS . . . . .	43
4.3	FRACTOGRAPH OF THE FATIGUE CRACK GROWTH SURFACE FOR THE 7075-T6 ALLOY . . . . .	44
4.4	FATIGUE CRACK PROPAGATION DATA FOR THE A1-10.2 WT Pct MG-0.52 WT PCT Mn ALLOY, SOLUTION TREATED FOR NINE HOURS . . . . .	45
4.5	FATIGUE CRACK PROPAGATION DATA FOR THE A1-10.2 WT PCT Mg-0.52 WT PCT Mn ALLOY, SOLUTION TREATED FOR TWENTY-FIVE HOURS . . . . .	46
4.6	SCANNING ELECTRON FRACTOGRAPH FOR THE NINE HOUR SOLUTION TREATED A1-10.2 WT PCT Mg-0.52 WT PCT Mn ALLOY . . . . .	47
4.7	SCANNING ELECTRON FRACTOGRAPH FOR THE TWENTY- FIVE HOUR SOLUTION TREATED A1-10.2 WT PCT Mg- 0.52 WT PCT Mn ALLOY . . . . .	48
4.8	OPTICAL MICROGRAPH FOR THE NINE HOUR SOLUTION TREATED A1-10.2 WT PCT Mg-0.52 WT PCT Mn ALLOY . . .	49
4.9	OPTICAL MICROGRAPH FOR THE TWENTY-FIVE HOUR SOLUTION TREATED A1-10.2 WT PCT Mg-0.52 WT PCT Mn ALLOY . . . . .	50

4.10 OPTICAL MICROGRAPH LOCATIONS FOR THE 9 AND 25 HOUR SOLUTION TREATED Mn CONTAINING ALLOYS, AND Cu CONTAINING ALLOYS. . . . .	51
4.11 FATIGUE CRACK GROWTH DATA FOR Al-8.14 WT PCT Mg-0.40 WT PCT Cu ALLOY . . . . .	52
4.12 SCANNING ELECTRON FRACTOGRAPH FOR THE Al-8.14 WT PCT Mg-0.40 WT PCT Cu ALLOY . . . . .	53
4.13 OPTICAL MICROGRAPH FOR THE Al-8.14 WT PCT Mg-0.40 WT PCT Cu ALLOY . . . . .	54

## ACKNOWLEDGMENT

I would like to take this opportunity to express my sincere thanks to those individuals who have given their support and guidance during the time span required to complete this study. I would like to thank Professor T.R. McNelley for his assistance as my advisor in organizing and conducting the experiments and in preparing the manuscript.

## I. INTRODUCTION

### A. PRIMARY PURPOSE

In recent years there has been an increasing emphasis on predicting the crack growth behavior in structural engineering materials. This is an outgrowth of the requirement that comprehensive crack growth data be obtained and interpreted accurately prior to structural design and manufacture. The primary purpose of this effort is to investigate the effects of thermomechanical processing and alloy content on aluminum magnesium alloys with eight and ten weight percent magnesium and additional alloying elements. Another purpose is to provide useful fatigue crack growth information, as well as a reliable method to obtain such data.

This study extends the knowledge obtained from the earlier efforts of Shirah {Ref. 1} and utilizes Johnson's {Ref. 2} and Cadwell's {Ref. 3} standardized thermomechanical process as a basis to process material for measurement of the fatigue crack growth rates of Al-10.2 wt pct Mg-0.52 wt pct Mn and Al-8.14 wt pct Mg-0.40 wt pct Cu alloys.

There are many methods used to measure crack growth in material specimens. All have distinct advantages and disadvantages with respect to accuracy, cost, and convenience of use. Fatigue crack growth measurements were accomplished using the optical method as outlined in Reference 4. The

optical method is the method of recording by an optical device the length of a crack breaking through the surface of a test specimen. This method is inexpensive and easy to initiate but very tedious. The method requires that a reliable operator take readings for the duration of the test. Tests can last for up to ten hours depending on the sample tested.

## B. BACKGROUND

The alloys processed in this report have higher magnesium content than the 5XXX series aluminum-magnesium alloys currently in use. These are considered wrought alloys and derive their strength through intermediate temperature thermomechanical processing. Conventional wrought 5XXX alloys contain up to six percent Mg and are low to medium strength alloys, possessing good corrosion resistance, fatigue resistance, ductility and weldability. Their strength, however, is considerably lower than the high strength alloys of the 7XXX type. The strength of such 5XXX alloys can be raised by adding more magnesium. By using conventional processing practices, however, numerous problems can arise, including increased stress corrosion susceptibility and difficulties in cold working (Ref. 5). A major reason for this is that upon quenching of the alloy, magnesium segregates to the grain boundaries or slip bands and the alloy behaves in a manner similar to sensitized stainless steel, with

decreased resistance to stress corrosion cracking. Therefore the 5XXX series alloys are generally limited to less than five weight percent magnesium.

In the processing method employed here {Ref. 2}, magnesium is precipitated during warm working. Warm working temperatures for purposes of this work are those from 200°C up to the solvus for Mg in the alloy. Under such working conditions, some Mg precipitation occurs but the precipitates are caused to be uniformly dispersed by the working rather than concentrated in grain boundaries and on slip bands. Strengthening results from development of dislocation structures during working, with magnesium still in solution, and some contribution due to the dispersed Mg-containing precipitates.

## II. EXPERIMENTAL PROCEDURES

### A. EQUIPMENT FABRICATION

The clevis assembly was designed to pull a two-pin tensile specimen as outlined in Reference 4. Due to premature failure of the test specimen in the pin region, the test specimens had to be redesigned. This also required a clevis design different from that required in Reference 4. The material selected for the clevis assembly was 4140 steel. The heat treatment procedure was in accordance with Reference 6: austentize at  $871^{\circ}\text{C}$  for one hour, oil quench and temper at  $482^{\circ}\text{C}$  for one hour. Both pieces were wrapped in nickel foil with titanium chips added to act as an oxygen getter. The clevis assembly was designed initially in accordance with Reference 8, but premature failure of the sample in the clevis region required re-design of the assembly as shown in Figure 2.1. The pins that were initially used in the clevis assembly were replaced with stainless steel bolts. By using the bolts in the clevis assembly it was possible to increase the normal force on the specimen surface, which distributed the load more uniformly, and the problem with premature failure at the clevis region was solved with no distortion of the bolt holes in the specimen during the fatigue test.

An alignment device was designed and fabricated to assure accurate alignment of the testing machine and specimen axis (Figure 2.2). The reference bar was held in place by two brackets which were machined from aluminum. Use of aluminum prevented damage to the load frame assembly when the alignment fixture was tightly secured (Figure 2.3). Both ends and the center of the reference bar were machined flat so that when the assembly was rigidly mounted all surfaces remained square. The center of the reference bar was calibrated in 3.175 mm (0.125 in) increments to facilitate the alignment procedure. A dial indicator was mounted on the bar and positioned so that full movement of the load cell could be measured. The load cell was moved horizontally to full left and right deflections in the crosshead and the readings were taken from the dial indicator. These readings were then added together and their sum halved to give the mean load cell position in the crosshead. This procedure was repeated several more times to verify the load cell was completely centered. To further verify the results of the dial indicator readings a machinist square was positioned on the center of the reference bar and a set of measurements was taken. This procedure insured that the material testing machine load cell was accurately aligned.

## B. MATERIAL PROCESSING

The alloys selected for this study were 7075-T6 alloy obtained from Kaiser Aluminum Co. in sheets with a thickness

of 1.27 mm (0.050 in) and two experimental alloys. The latter were obtained as direct chill cast ingots 127 mm (5 in) in diameter by 1060 mm (4 in) in length, produced by Alcoa Center for Technology, Pittsburgh, Penn. The as-received compositions of alloys are listed below in Table I.

Table I  
Table of Alloy Compositions

Serial	Si	Fe	Cu	Mg	Ti	Be	Mn
501300	0.03	0.03	0.00	10.2	0.01	0.002	0.52
501303	0.01	0.03	0.40	8.14	0.01	0.002	0.00

The as-received ingots were sectioned into billets 96 mm (3.75 in) long by 32 mm (1.25 in) square cross-section for subsequent thermomechanical processing (Figure 2.4).

Two different thermomechanical processes were employed for the Al-10.2 wt pct Mg-.052 wt pct Mn alloy. One process used a 9 hour solution treatment followed by hot upset forging and water quench, and the other, a 25 hour solution treatment followed by forging and quenching as before.

In the first method the billets were solution treated for 5 hours at 440°C and then 4 hours at 480°C. The billets were then isothermally upset forged from an initial height of 96 mm (3.75 in) to a final maximum height of 32 mm (1.25 in) to provide for hot work and break up the dendritic, as cast microstructure. After forging, the billets

received an additional one hour solution treatment at  $440^{\circ}\text{C}$  to insure subsequent quenching was from a completely solution treated condition. The billets were then quenched to room temperature, with water as the quenching medium. In the second method, the billets were solution treated for 21 hours at  $480^{\circ}\text{C}$ , isothermally forged at  $440^{\circ}\text{C}$ , and given an additional one hour solution treatment at  $440^{\circ}\text{C}$ . Again, water was used as the quenching medium. The copper containing alloy was solution treated for 4 hours at  $440^{\circ}\text{C}$ , isothermally forged at  $440^{\circ}\text{C}$  with an additional one hour of annealing at  $440^{\circ}\text{C}$ , followed by a water quench. The final dimensions at the conclusion of the forging process were the same as outlined for the previous alloy.

The forged billets were further deformed by the warm rolling procedure reported by Johnson {Ref. 2}. A warm rolling temperature of  $300^{\circ}\text{C}$  was selected to facilitate comparison with the data of Johnson {Ref. 2} and Cadwell {Ref. 3}. The warm rolling was accomplished by first heating the billets to the rolling temperature. This required that the billets be placed in a preheated furnace for ten minutes prior to the first pass through the rolling mill. Since the mill rolls were not heated, consideration had to be given to the temperature loss which would occur during each rolling pass. To compensate for this temperature drop the billets were reheated for an average of seven minutes between passes. To maintain the straightness of the

billet, a four-pass sequence was utilized as outlined by Johnson (Ref. 2), (Figure 2.5). The final thickness was 3.6 mm (0.140 in) in all cases, and an as-rolled sample is shown in Figure 2.6.

Following rolling, the billets (Figure 2.7) were machined in accordance with Reference 4. Premature cracking in the area of the pinhole of the sample was noted in crack growth measurements and this required a design modification (Figure 2.8). The final design for the crack initiator notch was chosen after several crack growth measurements were performed using the 7075-T6 alloy test material. This consisted of drilling a 4.98 mm (0.196 in) hole in the center of the specimen and then making a saw cut out from both sides of the hole. The sawcuts were required to be accurate to ensure that they were square with the sample ends. This ensured that the load distribution was symmetrical with respect to the specimen notch. The details of the crack initiator notch geometry are shown in Figure 2.9; also of note is the 30 degree crack angle at the notch tip, also shown in Figure 2.9.

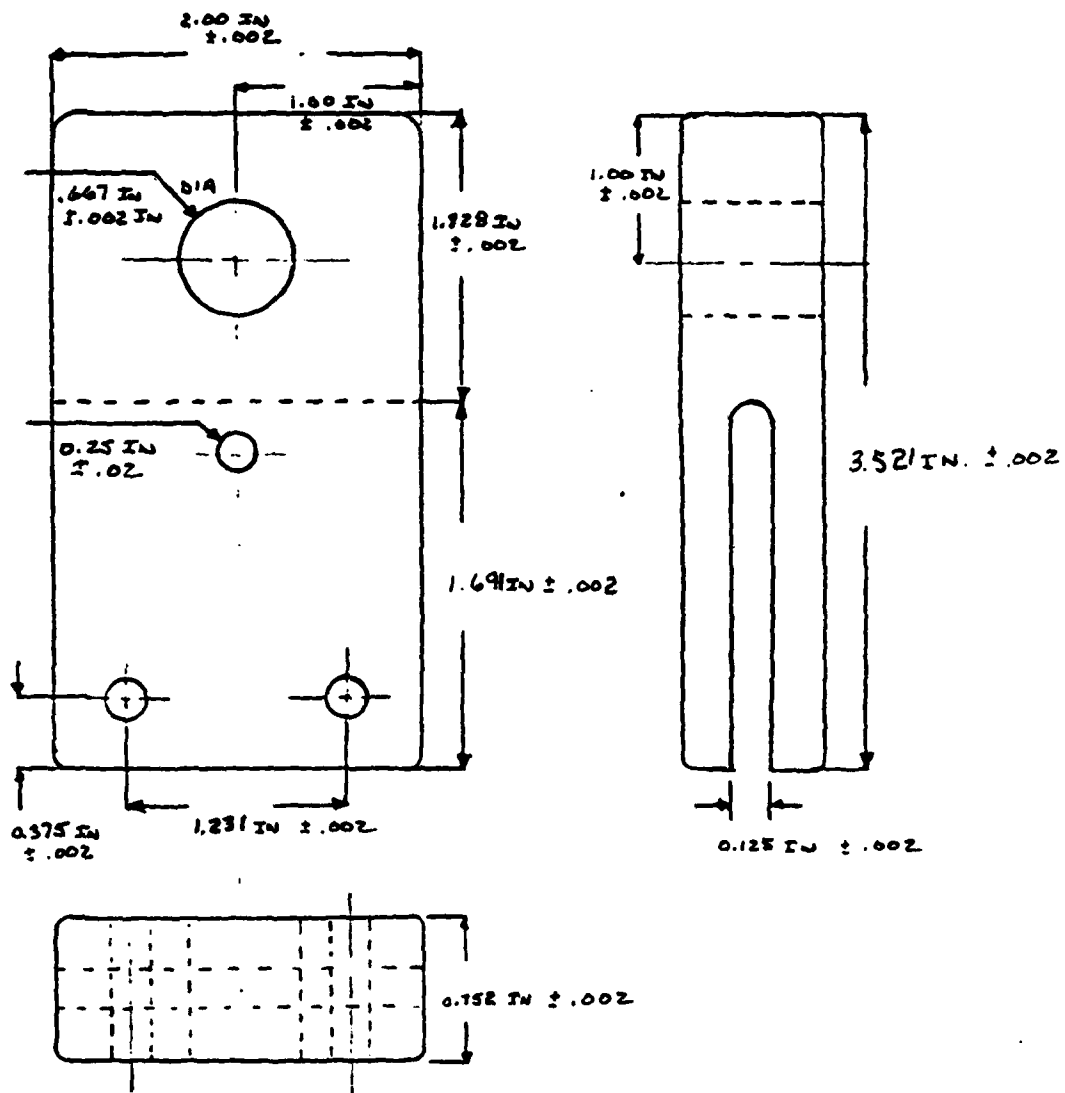


FIGURE 2.1 . DIAGRAM OF CLEVIS ASSEMBLY FABRICATED FROM 4140 STEEL

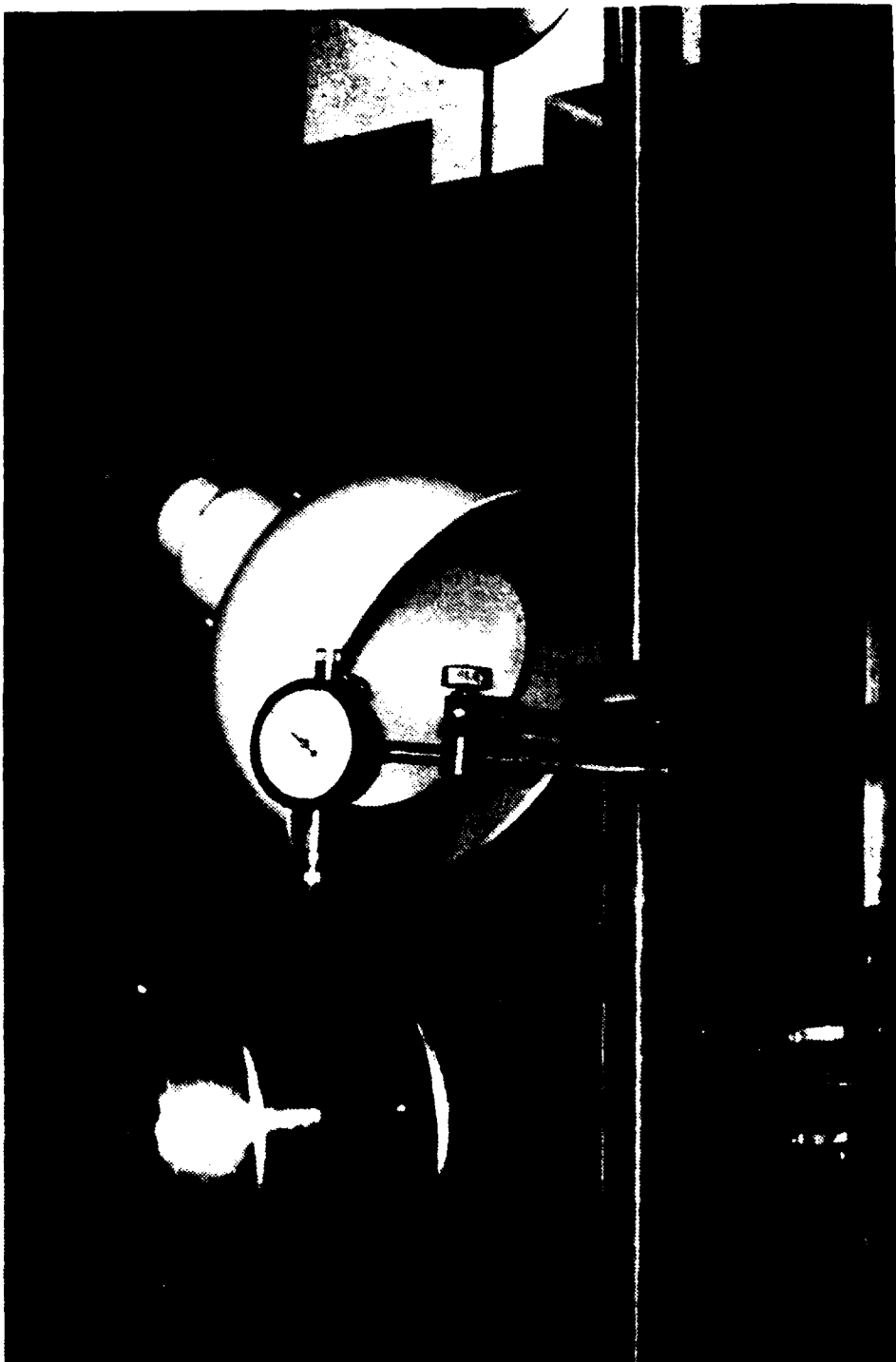


FIGURE 2.2 THE ALIGNMENT APPARATUS AS MOUNTED ON THE MTS MACHINE SHOWING THE DIAL INDICATOR AND LOAD CELL, DURING CENTERING OF LOAD CELL. THE GRIPS AND HYDRAULIC RAM ARE BELOW THE BAR.

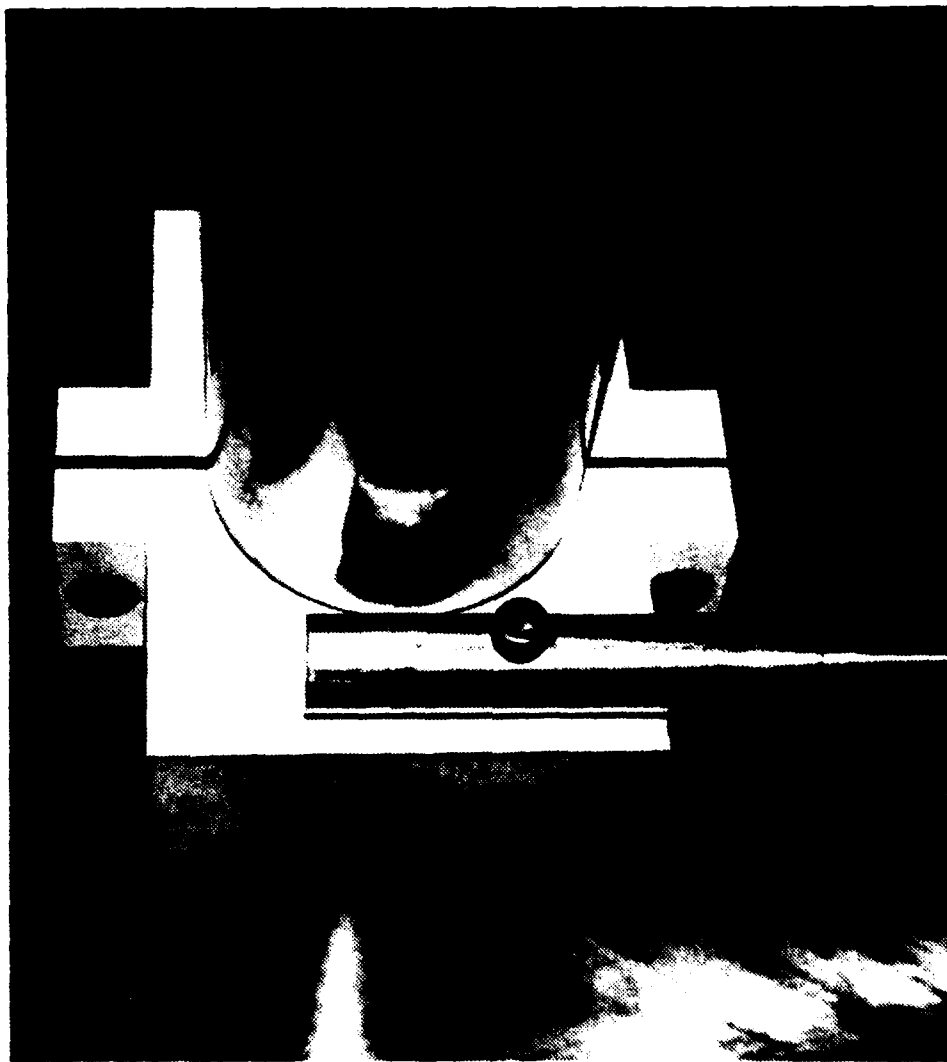


FIGURE 2.3 THE ALIGNMENT BAR CLAMP AS MOUNTED ON THE LEFT  
SIDE OF THE LOAD FRAME ASSEMBLY CONSTRUCTED OF ALUMINUM  
AND SUPPORTING STEEL ALIGNMENT BAR

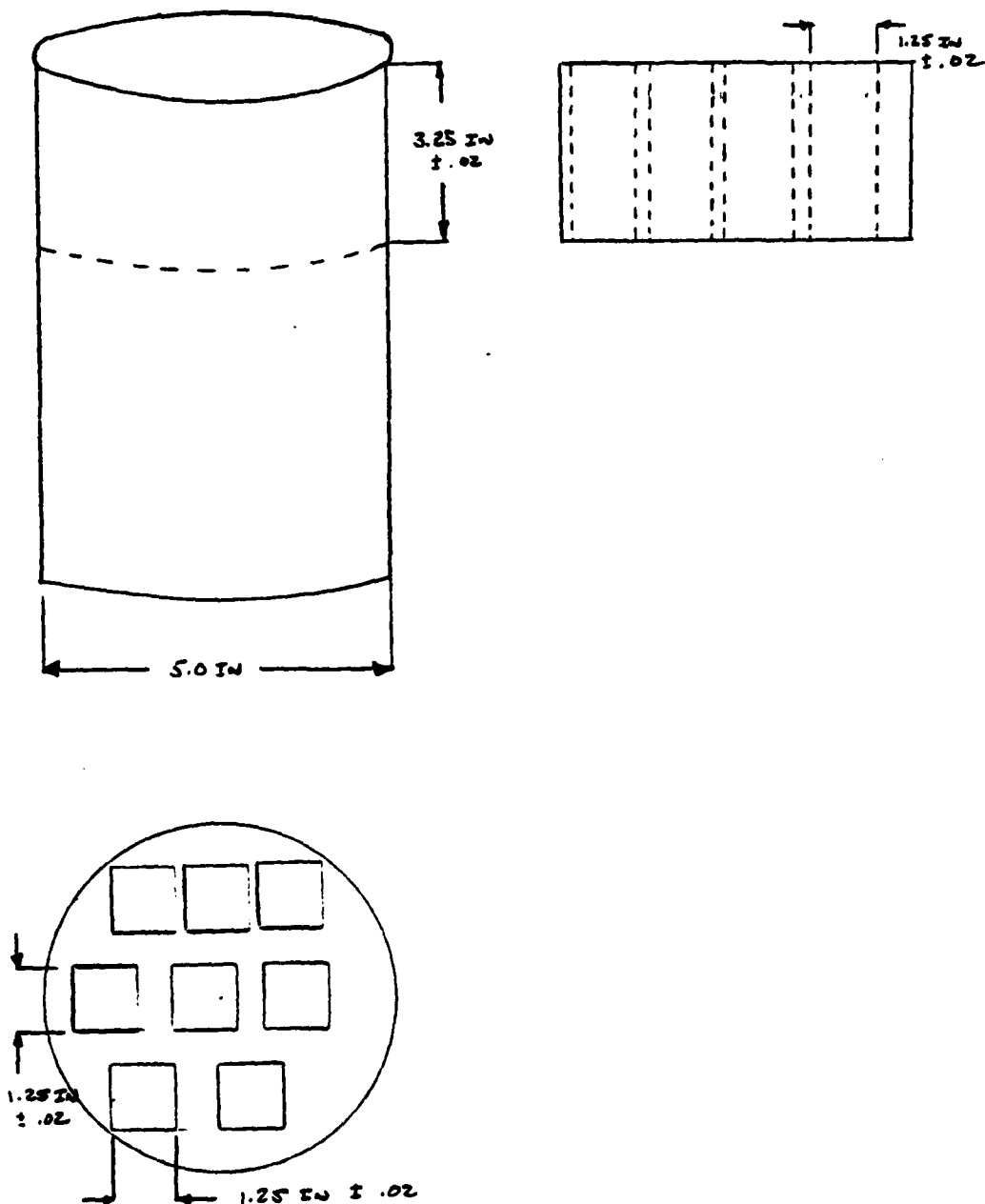


Figure 2.4 DIAGRAM SHOWING THE SECTIONING OF THE AS-CAST INGOT TO OBTAIN BILLETS FOR THERMO-MECHANICAL PROCESSING.

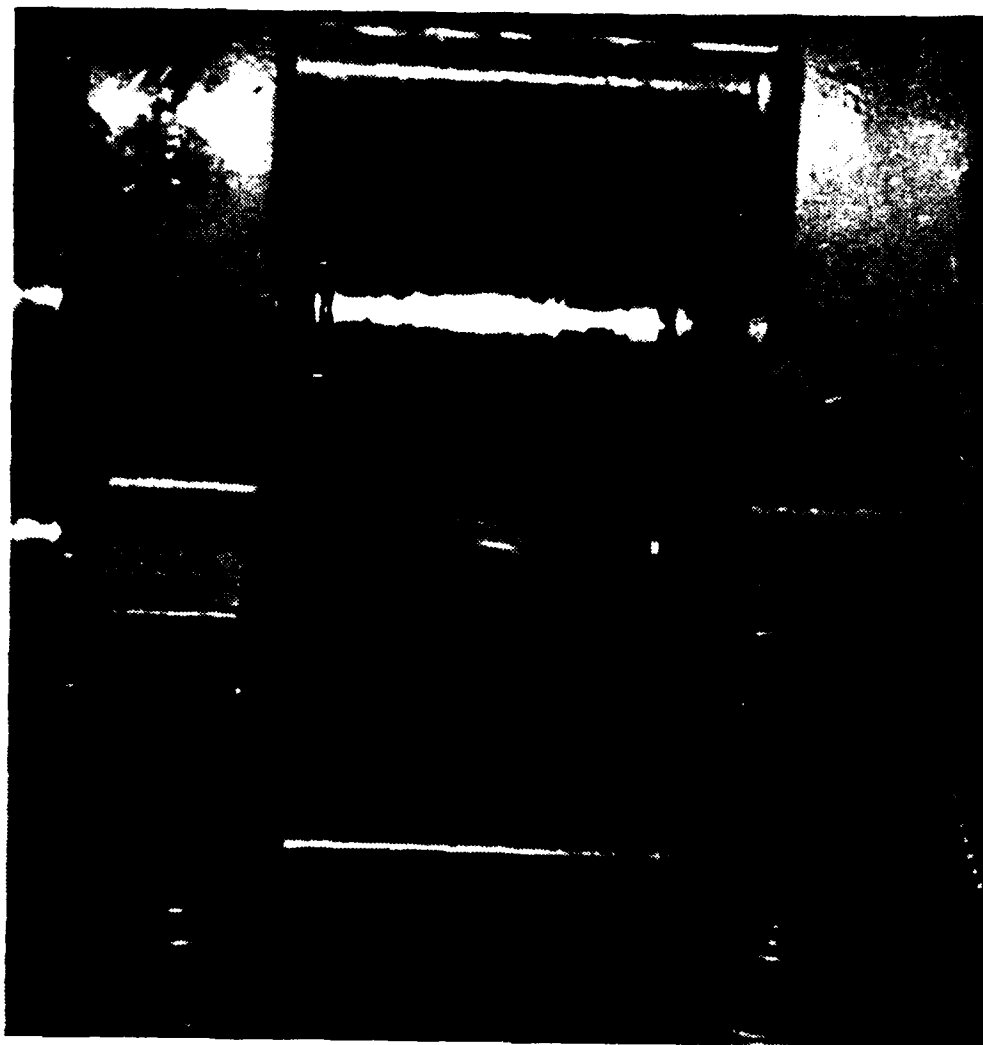


FIGURE 2.5 A ROLLING BILLET ON THE RUN IN  
THE TABLE OF THE ROLLING MILL



Figure 2.6 AN AS-ROLLED SAMPLE OF Al-10.2 Wt PCT Mg-  
0.52 Wt PCT Mn ALLOY; SAMPLE WIDTH IS APPROXIMATELY  
THREE INCHES.



Figure 2.7 ORIGINAL DESIGN OF MACHINED SPECIMEN WITH  
LARGE PIN-HOLES AT EACH END TO FIT IN THE  
CLEVIS ASSEMBLY

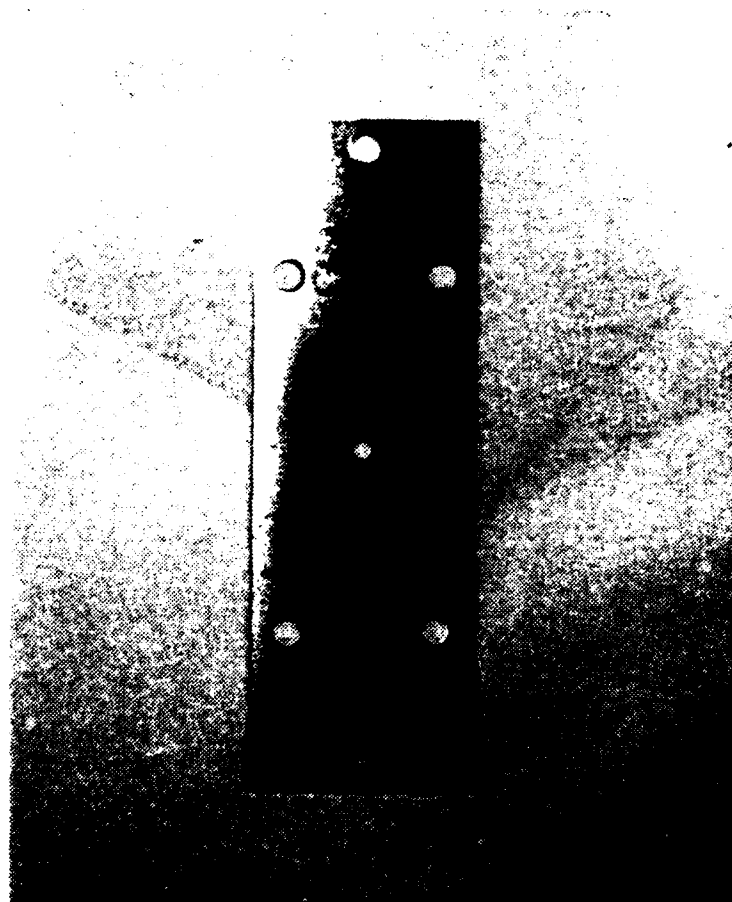


Figure 2.8 REDESIGN OF MACHINED SPECIMEN. THREE  
SMALLER HOLES WERE SUBSTITUTED FOR LARGER PIN-  
HOLES IN ORIGINAL DESIGN.

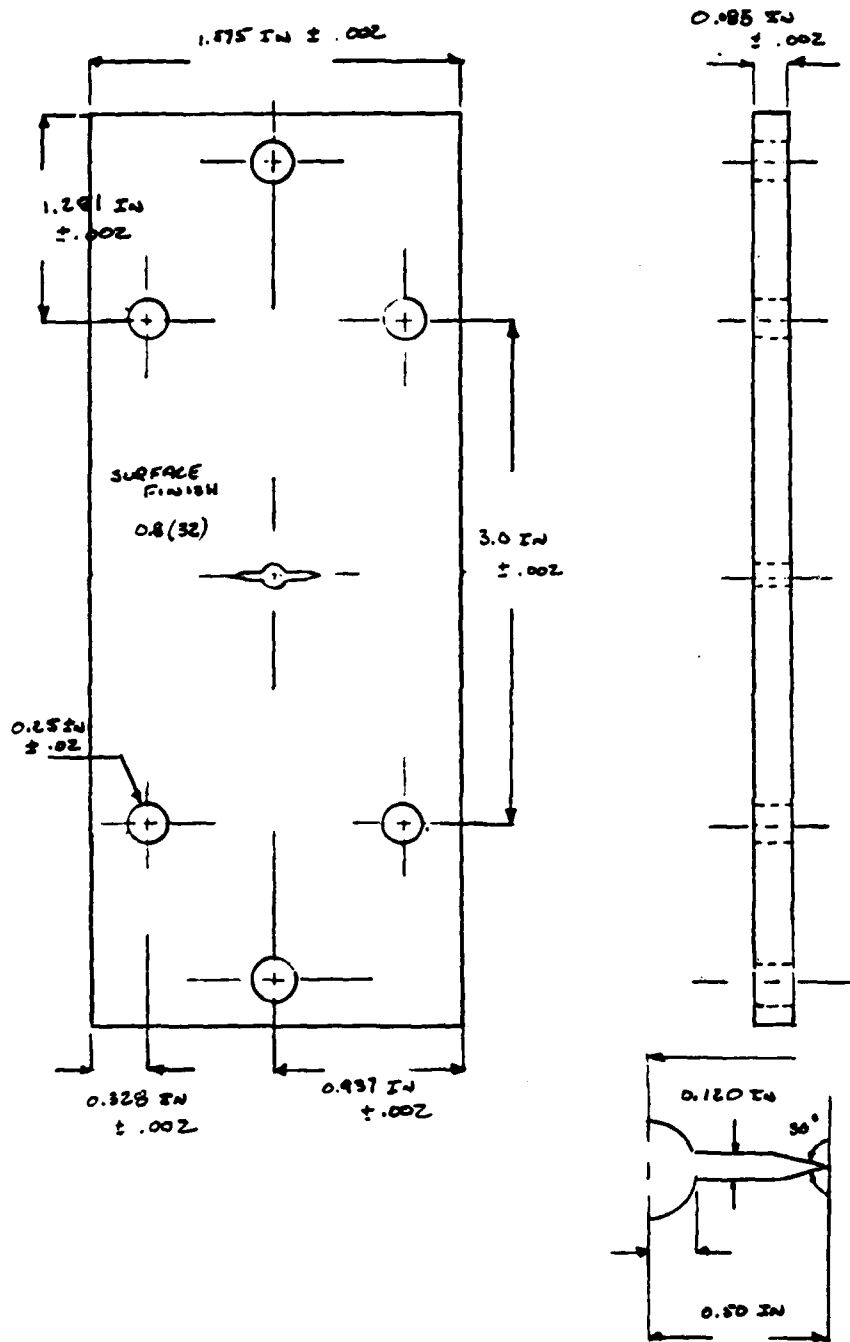


Figure 2.9 SCHEMATIC DIAGRAM OF THE FINAL DESIGN OF THE CENTER-CRACK TENSION TEST SPECIMEN USED FOR FATIGUE CRACK GROWTH MEASUREMENT.

### III. FATIGUE CRACK GROWTH MEASUREMENT

#### A. MEASUREMENT TECHNIQUE

All fatigue crack growth measurements reported here were made using an MTS Model 810 servo-hydraulic testing machine. To conduct a test, the load cell was aligned using the fixture described previously. The specimen was then installed in the machine using the clevis assembly. In some cases, the specimens were not flat; however, the fifty pound preload applied prior to testing corrected the curvature and this was checked using an engineer's square.

A haversine waveform was selected from the digital function generator of the MTS machine. This, with the fifty pound pre-load ensured that a tensile load was applied to the specimen at all times. Fatigue crack length measurements were made as a function of elapsed cycles by means of an optical device shown in Figure 3.2. This was used following the procedures as outlined in Reference 7. The device consists of a Bausch and Lomb 22.7 mm, 6X telescope in conjunction with a Nikon 86 mm zoom lens. The surface of the specimen was sprayed with steel blue layout fluid to make the crack more visible. Reference marks were applied in .381 mm (0.015 in) divisions from the notch tip to the edge of the sample. By using a stationary optical device and reference marks as opposed to a

traveling microscope as outlined in literature, potential errors due to accidental movement of the traveling microscope were eliminated {Ref. 7}.

Crack length measurements were made at intervals such that the crack growth rate was determined at equal increments in the stress intensity range,  $\Delta K$ .  $\Delta K$  was calculated using the following expression:

$$\Delta K = \frac{\Delta P}{B} \sqrt{\frac{\pi \alpha}{2w}} \sec \frac{\pi \alpha}{2}$$

Where the terms are defined as follows:

- $\Delta K$  =  $P_{\max} - P_{\min}$
- $\alpha$  =  $2a/w$
- $b$  = thickness
- $w$  = width
- $a$  = pre-crack length

Data reduction was accomplished using the two Fortran programs shown in Appendices A,B. The analysis technique involved was the modified secant method. Data reduction was done in two steps. First, the raw data was taken from the optical device and the test machine cycle counter and entered into the interactive Fatigue 1 program. After the entries in Fatigue 1 were checked, an input file was automatically generated and loaded into the Fatigue 2 program. Second, the Fatigue 2 program was then used to generate the final output data and associated graphs of  $da/dn$  vs.  $\Delta K$ .

## B. TENSILE TESTING

Tension testing was accomplished using samples machined to non-standard form necessitated by the limited material availability. The testing was accomplished utilizing an Instron model TT-D floor model testing machine with a crosshead speed of 5 mm (0.2 in) per minute. Load elongation data were autographically recorded.

## C. METALLOGRAPHY

All sample mounting for metallographic examination was done using room temperature epoxy resin compounds, and all cutting was done by wet cutting methods. Polishing of the specimens involved wet sanding with 240, 300, 400 and 600 grit paper with further polishing using a magnesium oxide (Magomet) slurry. This slurry was put on a polishing wheel (Automet) and distilled water was applied while the polishing was done. The etchant used was Barker's reagent as outlined in Reference 8. All photomicrographs were taken using a Zeiss optical microscope.



FIGURE 3.1 SPECIMEN MOUNTED IN THE CLEVIS ASSEMBLY; CHECK FOR ALIGNMENT  
USES THE DIAL INDICATOR; ABOVE IS THE LOAD CELL AND BELOW IS  
THE HYDRAULIC RAM

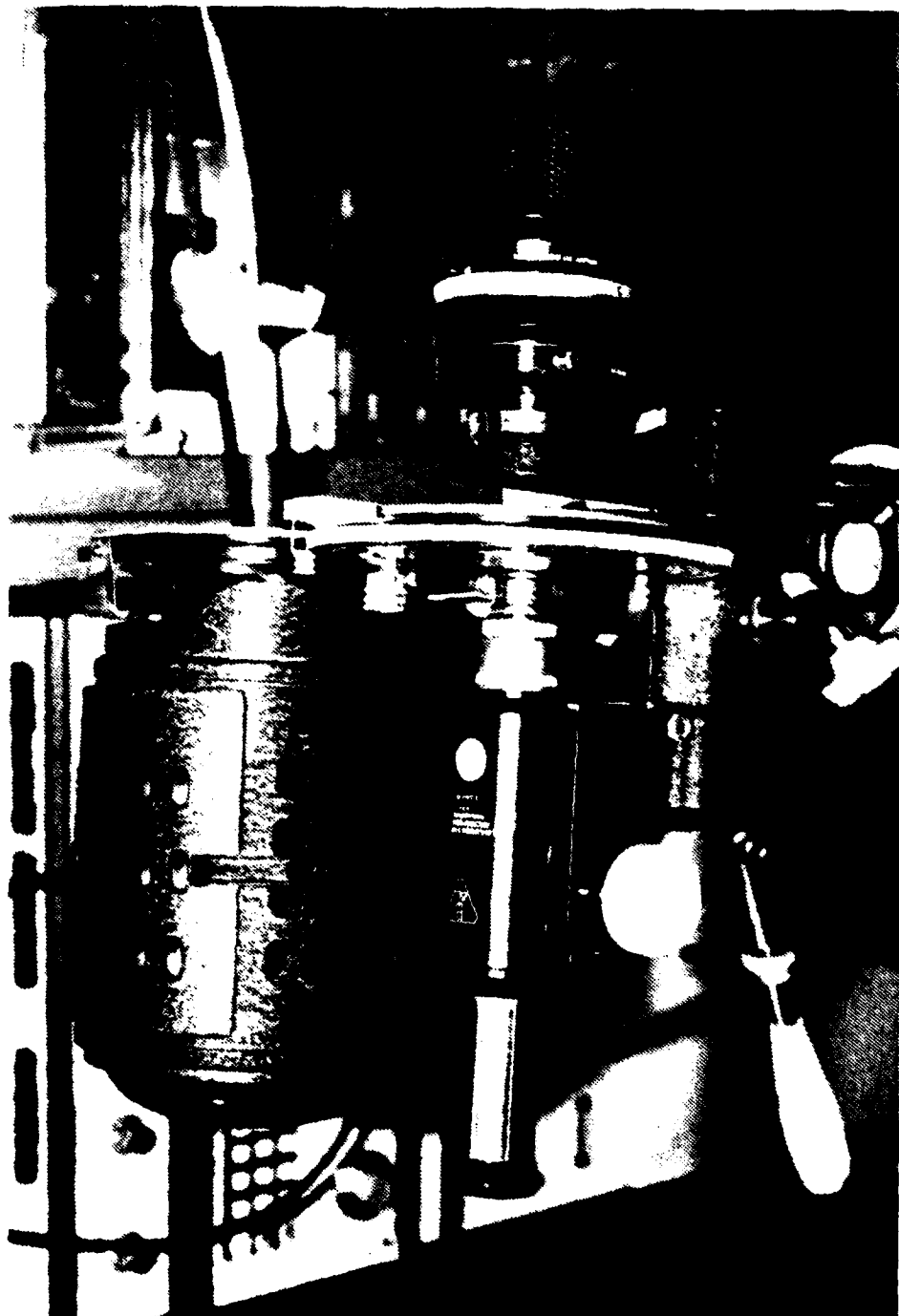


FIGURE 3.2 OPTICAL DEVICE USED TO MEASURE CRACK LENGTH, A BAUSCH & LOMB  
22.7 MM, 6X TELESCOPE IN CONJUNCTION WITH A HEON 86 MM 300X LENS

#### IV. RESULTS AND DISCUSSION

##### A. MATERIAL PROCESSING

The thermomechanical material processing scheme developed by Johnson {Ref. 2} and modified by Cadwell {Ref. 3} was followed closely to facilitate comparison with previous work. No major difficulties were encountered in processing the Al-10.2 wt pct Mg-0.52 wt pct Mn alloy. It was found however, that severe cracking did occur on some of the Al-8.14 wt pct Mg-0.42 wt pct Cu alloy billets. The cracking was layered in appearance and appeared to be intergranular. Cadwell {Ref. 3} had also reported this behavior. By reducing the rolling reduction to 0.508 mm (0.020 in) per-pass the problem was eliminated. Using this modified rolling procedure a sufficient amount of material was processed for the number of fatigue specimens required.

##### B. RESULTING TENSILE PROPERTIES

The results of the tension testing generally agreed with the results reported by Cadwell {Ref. 3} and Shirah {Ref. 1}. The ultimate tensile strength of the Al-10.2 wt pct Mg-0.52 wt pct Mn alloy, solution treated for nine hours, was 67 ksi (462 MPa). This was slightly lower than the 70 ksi (487 MPa) value obtained by Shirah {Ref. 1}

and Cadwell {Ref. 3}. The Al-10.2 wt pct Mg-0.52 wt pct Mn alloy solution treated for twenty-five hours showed an ultimate tensile strength of 63 ksi (434 MPa) which was also lower than results reported earlier. The Al-8.14 wt pct Mg-0.40 wt pct Cu alloy had an ultimate tensile strength of 60 ksi (414 MPa), again slightly lower than the 65 ksi (448 MPa) reported earlier. It is not known why results obtained here are generally three to five ksi below those reported previously {Refs. 1,3} but it should be noted again that nonstandard test geometries were used here, whereas ASTM standard geometry samples were employed in the previous work.

#### C. FATIGUE CRACK PROPAGATION 7075-T6 ALLOY

The 7075-T6 alloy was chosen for initial testing due to the availability of well documented data for comparison and validation of test procedures, and also the local availability of the material in large quantities. The crack growth data obtained for this material as shown in Figure 4.1,  $\Delta k$  and follows closely the data reported in Reference 9.

##### 1. Scanning Electron Microscopy

Fatigue crack surfaces were examined by scanning electron microscopy (SEM). Fractograph locations for all SEM work are shown in Figure 4.2 and fractographs of the 7075-T6 alloy are shown in Figure 4.3. Observed in the fractographs are small "dimples", microvoids and crack

ridges. The appearance of the crack surface follows very closely that described in Reference 10 for 7075-T6 and indicates that a uniaxial load was applied to the test specimen. The voids observed were probably nucleated by iron and silicon-rich second phase particles present in the alloy. It has been proposed by Reference 9 that the presence of these compounds in the alloy causes a reduction in fracture toughness.

#### D. FATIGUE CRACK PROPAGATION MANGANESE CONTAINING ALLOY

The crack propagation data obtained for the nine hour solution treated Al-10.2 wt pct Mg-0.52 wt pct Mn alloy (Figure 4.4) shows it to be less fatigue crack growth resistant than the 7075-T6 alloy. The alloys appear to have similar threshold values of  $\Delta K$ , about  $7.5 \text{ ksi } \sqrt{\text{in}}$ , below which the crack growth rate decreases rapidly. The twenty-five hour solution treated Al-10.2 wt pct Mg-0.52 wt pct Mn alloy shows an even further degradation in the fatigue crack growth resistance compared to that of the nine hour solution treated alloy as shown in Figure 4.5.

##### 1. Scanning Electron Microscopy (SEM)

Scanning electron microscopy was conducted on both the nine- and twenty-five hour solution treated alloys and the results are shown in Figures 4.6 and 4.7. The fracture surfaces appear similar, with the twenty-five hour solution

treated alloy showing somewhat greater toughness than the nine hour solution treated alloy. The predominant feature of the fractographs of both alloys are small, shallow, closely-spaced dimples. The shallowness of the dimples reflects little tendency for void growth, and is indicative of a low ductility alloy. Also, there appear to be some precipitate particles, three to four microns in size, on the surface.

The large population of small micro-voids suggest many nucleation sites for such voids and little opportunity for them to grow. This would lead to a small plastic zone and a ready crack growth mechanism. The appearance of these micro-voids over the entire fracture surface indicates that the cracking process occurred by local tensile overload at the crack tip, and crack growth was by the nucleation and link-up of the small micro-voids in the structure. This is reflected in the ready crack growth exhibited by these alloys and low apparent fracture toughness.

## 2. Transmission Electron Microscopy

Transmission electron microscopy (TEM) examination of these alloys is being conducted concurrently in this laboratory, but is not part of this work. Reference 11 indicates that the microstructure of this Al-10.2 wt pct Mg-0.52 wt pct Mn alloy consists of elongated grains with a fine subgrain structure. The subgrain boundaries

appear to be associated with fine  $Mn Al_6$  precipitates 0.1 to 0.5 microns in size, and to a lesser extent with relatively large "beta" ( $Mg_5 Al_8$ ) particles. If comparisons are made between the material solution treated for twenty-five hours and solution treated for nine hours, the  $Mn Al_6$  particles are more numerous and larger in the material solution treated for the longer period of time. This would suggest that they are not dissolved during solution treatment as previously thought (based on optical microscopy). Rather, the  $Mn Al_6$  is insoluble and precipitates in increasing amounts during solutioning of the magnesium. The solid solution is supersaturated with manganese given the relatively rapid cooling rates that are associated with the direct chill casting method employed in the manufacture of these ingots, thus allowing the Mn to precipitate. The amount of "beta" precipitated in subsequent warm rolling is about the same for both alloys. Thus, it would appear that the  $Mn Al_6$  phase and its coarsening is responsible for the reduction of the fatigue crack resistance of the Al-10.2 wt pct Mg-0.52 wt pct Mn alloy.

### 3. Optical Microscopy

Optical micrographs of the nine hour and twenty-five hour solution treated alloys are shown in Figures 4.8 and 4.9 respectively. The relative locations of the micrographs with respect to the crack surface are shown in Figure 4.10. There is little difference in the micrographs between the two

materials although the twenty-five hour solution treated alloy does show slightly more precipitation than the nine hour solution treated alloy. In neither alloy is there any indication of a grain structure, however, there is considerably more precipitation than in the copper containing alloy discussed later.

#### E. FATIGUE CRACK PROPAGATION IN THE COPPER CONTAINING ALLOY

Fatigue crack growth data for the Al-8.14 wt pct Mg-0.40 wt pct Cu alloy are presented in Figure 4.11. The data for this alloy indicates a higher threshold stress intensity ( $\Delta = 10 \text{ ksi } \sqrt{\text{in}}$ ) for fatigue crack growth than either the 7075-T6 or Al-10.2 wt pct Mg-0.52 wt pct Mn alloys. At higher stress intensity values, crack growth rates for this alloy are much reduced in comparison to the manganese containing alloy and are also lower than those measured for the 7075-T6 in this research. Crack growth rates were measured at  $\Delta$  values up to  $30 \text{ ksi } \sqrt{\text{in}}$ , where the growth rate measured was approximately  $3 \times 10^{-5} \text{ in/cycle}$ . This reflects a higher degree of toughness in this alloy. It must also be noted, however, that this is the lowest strength material of the three different compositions evaluated in this research and is certainly a factor in the higher apparent toughness of this alloy. At this point, the appropriate strength toughness data has not been obtained to facilitate comparison of these alloys amongst themselves or with conventional alloys.

## 1. Scanning Electron Microscopy

Scanning electron microscopy (SEM) investigation of this alloy was conducted and the results appear in Figure 4.12. The fatigue crack surface is similar in general appearance to that of the 7075-T6 alloy. There are, however, two important differences. First, the Al-8.14 wt pct Mg-0.40 wt pct Cu alloy exhibits sharply defined ridges parallel with the direction of crack growth and second, there do not appear to be any large dimples in this alloy. The ridges correspond to grain boundaries and suggest that the crack front tends to split such that the crack does not remain planar.

## 2. Optical Microscopy

The optical micrographs (Figure 4.13) indicate the presence of flattened elongated grains. The tendency of the crack to split onto different planes would retard crack growth but the elongated grain structure would suggest that this enhancement in crack growth resistance would not be isotropic. The dimples on the 7075-T6 fracture surfaces are probably the result of voids nucleation at large constituent particles associated with the Fe and Si present in this alloy. The Fe and Si content in this alloy is much lower than that of 7075-T6 and hence the constituent particles are not present to be associated with such void formation.

### 3. Transmission Electron Microscopy

Transmission electron microscopy (TEM) (Ref. 12) of this alloy has indicated a considerable difference exists between this alloy and the manganese-containing alloy. In the as-rolled condition, this copper containing alloy exhibits elongated grains with a diffuse distorted cell structure and a lesser extent of beta precipitation. The beta precipitation has occurred principally in the grain boundaries, and there does appear to be some additional particles not associated with the dislocation cell structure; these latter are perhaps particles of a copper-containing phase. The fine, shallow dimples noted on the fracture surface of the manganese containing alloy were suggested to be associated with the presence of a manganese containing dispersoid. The absence of such a dispersoid in this copper containing alloy and the absence of such fine microvoid formation would tend to confirm this conclusion. However, the amount of beta precipitation also differs and it would be necessary to control both the presence of the beta and the additional dispersoids to obtain unambiguous data on the importance of the various precipitated phases in these alloys.

FATIGUE CRACK PROPAGATION BEHAVIOR 7075-T6

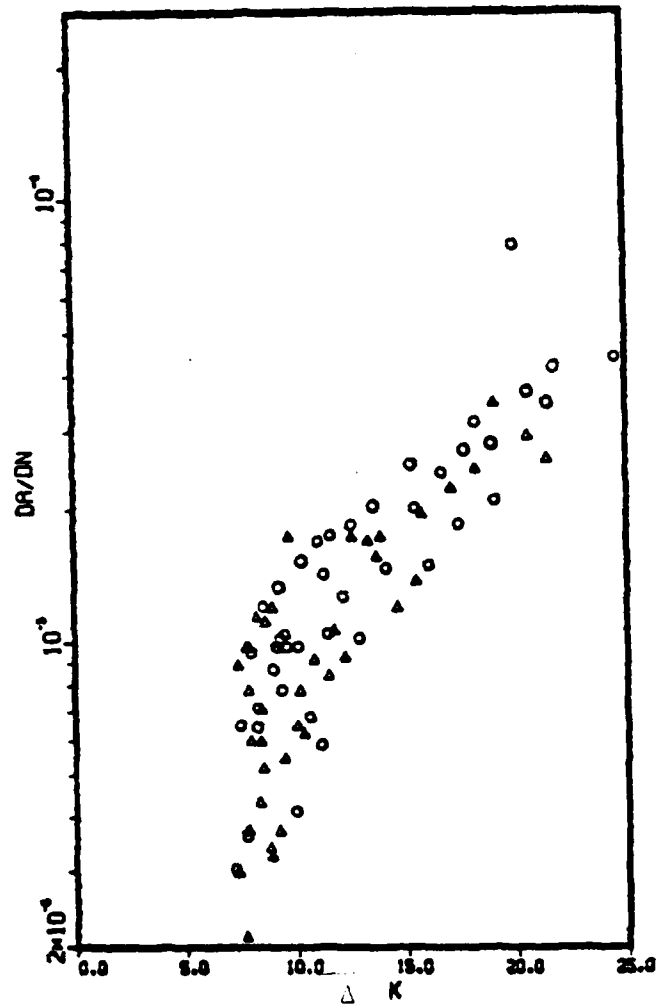


FIGURE 4.1 FATIGUE CRACK PROPAGATION DATA FOR 7075-T6 ALLOY

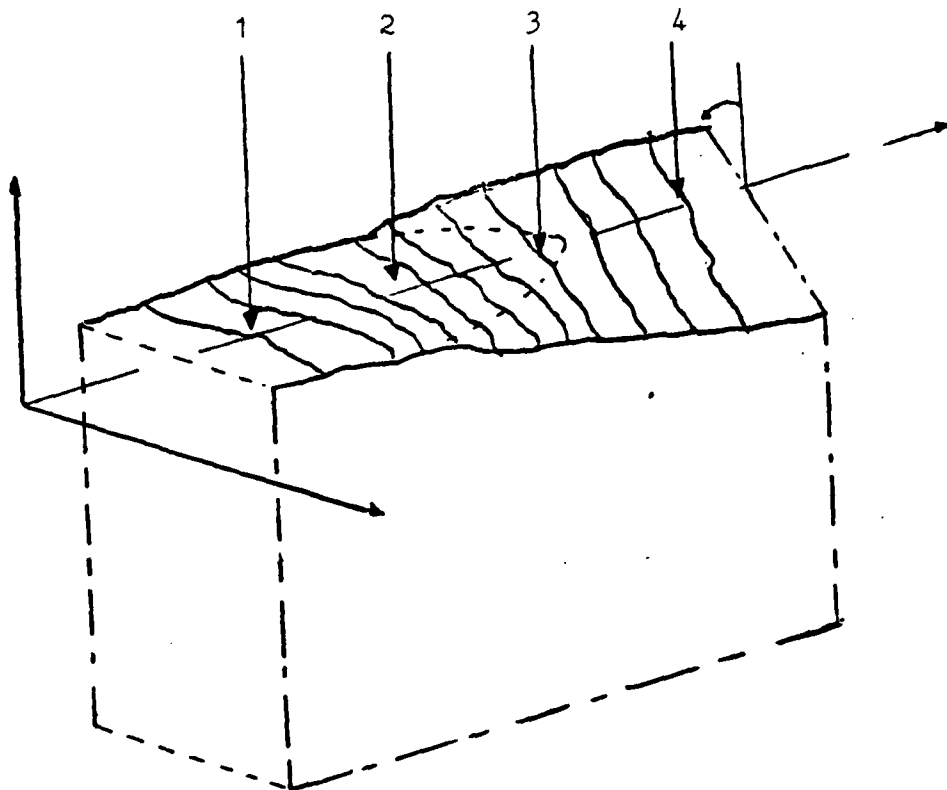


FIGURE 4.2 A SCHEMATIC SHOWING SCANNING ELECTRON MICROGRAPH LOCATIONS ON THE FATIGUE CRACK SURFACE FOR THE 7075-T6 AND THE MANGANESE, AND COPPER CONTAINING ALLOYS



FIGURE 4.3    FRACTOGRAPH OF THE FATIGUE CRACK GROWTH SURFACE  
FOR THE 7075-T6 ALLOY

# FATIGUE CRACK PROPAGATION BEHAVIOR 300A

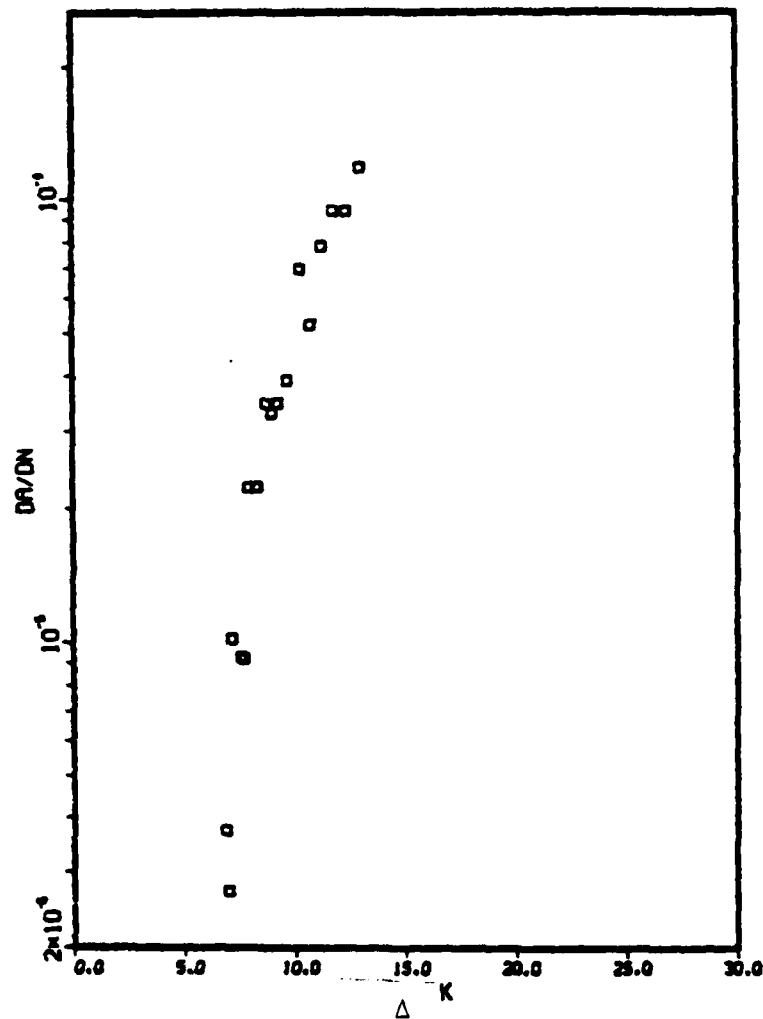


FIGURE 4.4 FATIGUE CRACK PROPAGATION DATA FOR THE Al-10.2  
WT PCT Mg-0.52 WT PCT Mn ALLOY SOLUTION TREATED FOR NINE HOURS

# FATIGUE CRACK PROPAGATION BEHAVIOR 300A

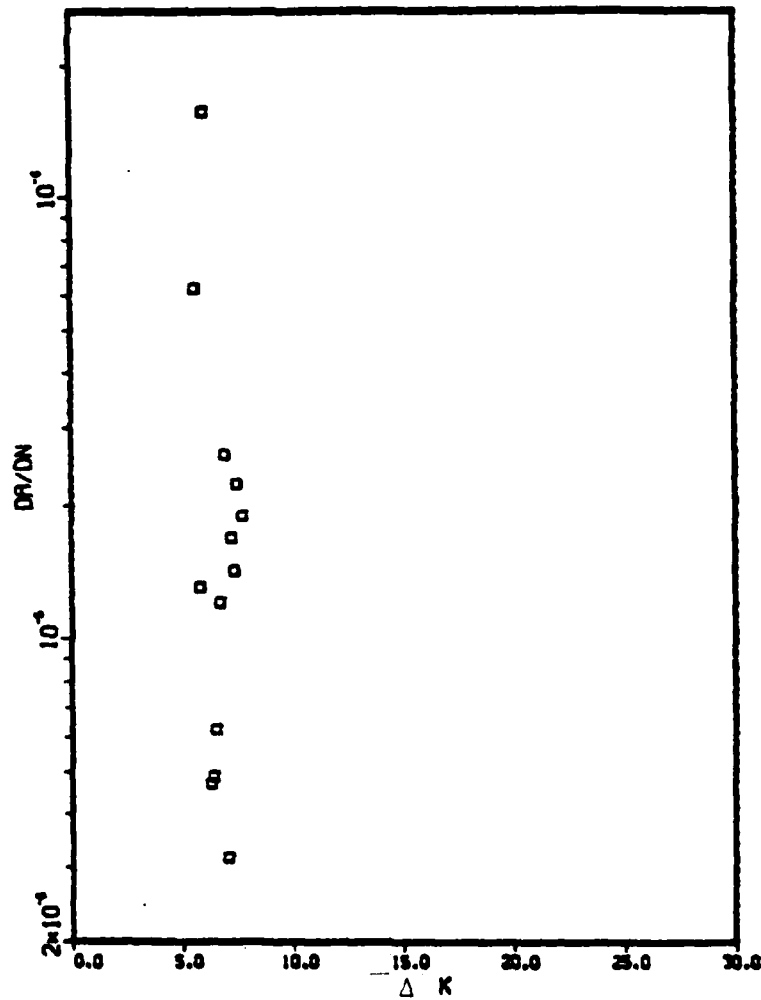


FIGURE 4.5 FATIGUE CRACK PROPAGATION DATA FOR THE Al-10.2  
WT PCT Mg-0.52 WT PCT Mn ALLOY SOLUTION TREATED  
FOR TWENTY-FIVE HOURS.

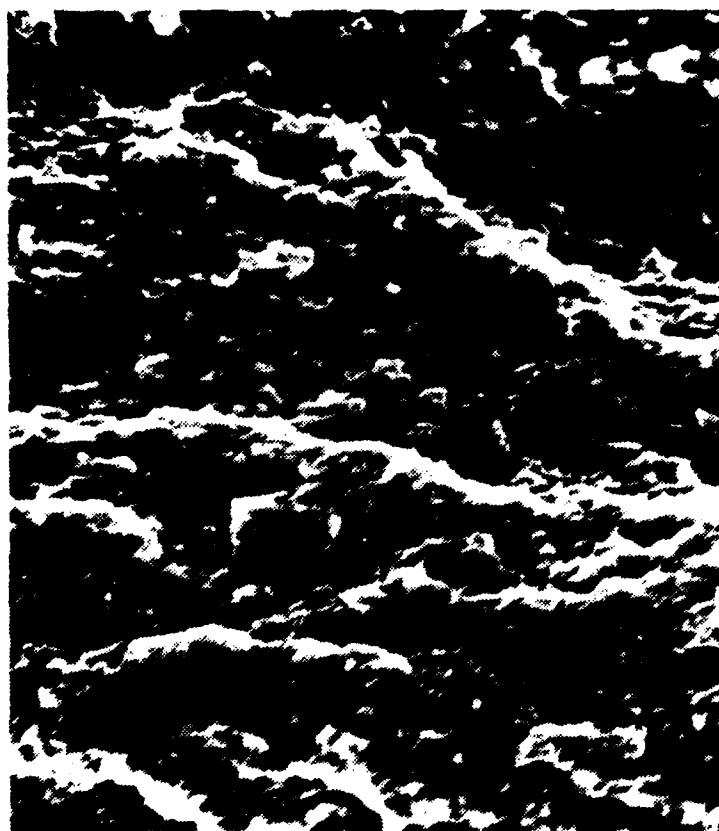


FIGURE 4.6 SCANNING ELECTRON FRACTOGRAPH FOR THE NINE HOUR  
SOLUTION TREATED Al-10.2 WT PCT Mg-0.50 WT PCT Mn ALLOY

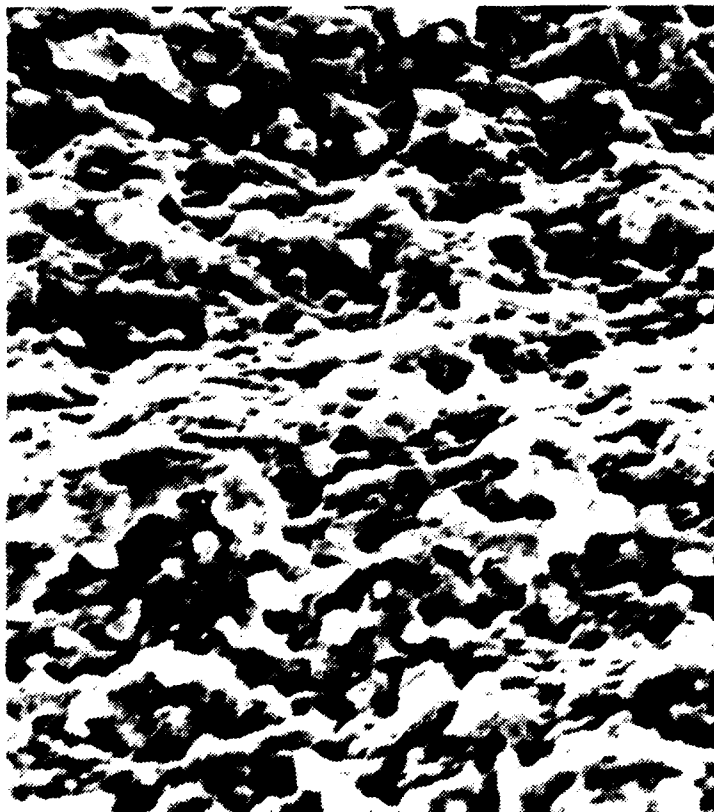


FIGURE 4.7 SCANNING ELECTRON FRACTOGRAPH FOR THE TWENTY-FIVE  
HOUR SOLUTION TREATED Al-10.2 WT PCT Mg-0.52 WT PCT Mn ALLOY

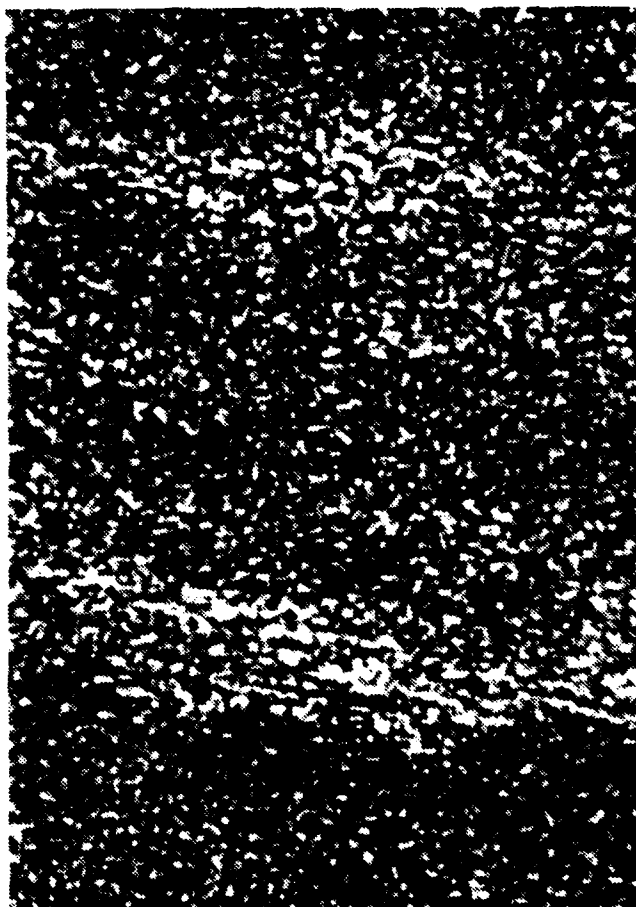


FIGURE 4.8 OPTICAL MICROGRAPH FOR THE NINE HOUR SOLUTION  
TREATED Al-10.2 WT PCT Mg-0.52 WT PCT Mn ALLOY.

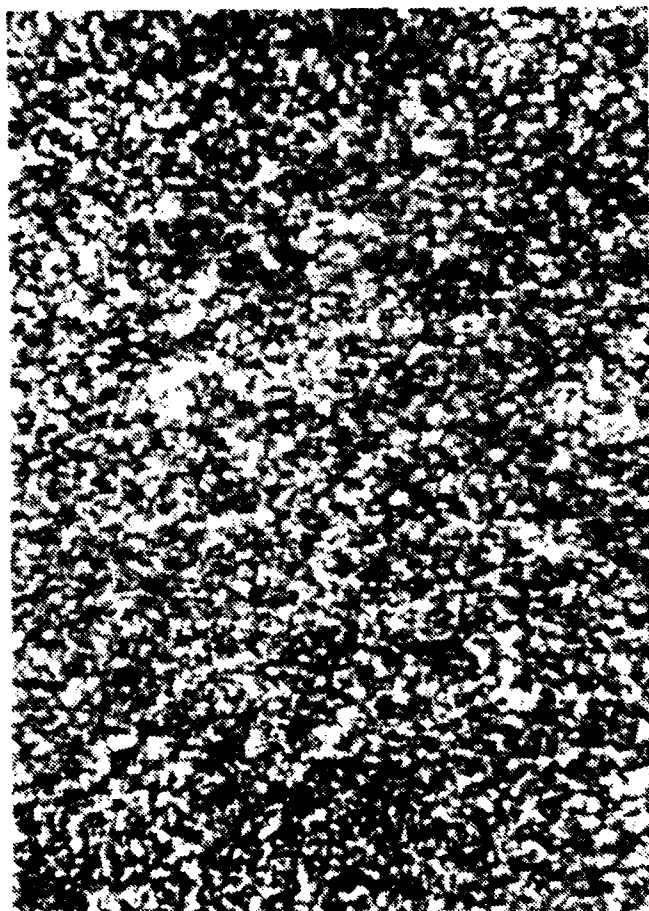


FIGURE 4.9 OPTICAL MICROGRAPH FOR THE TWENTY-FIVE HOUR  
SOLUTION TREATED Al-10.2 WT PCT Mg-0.52 WT PCT Mn ALLOY

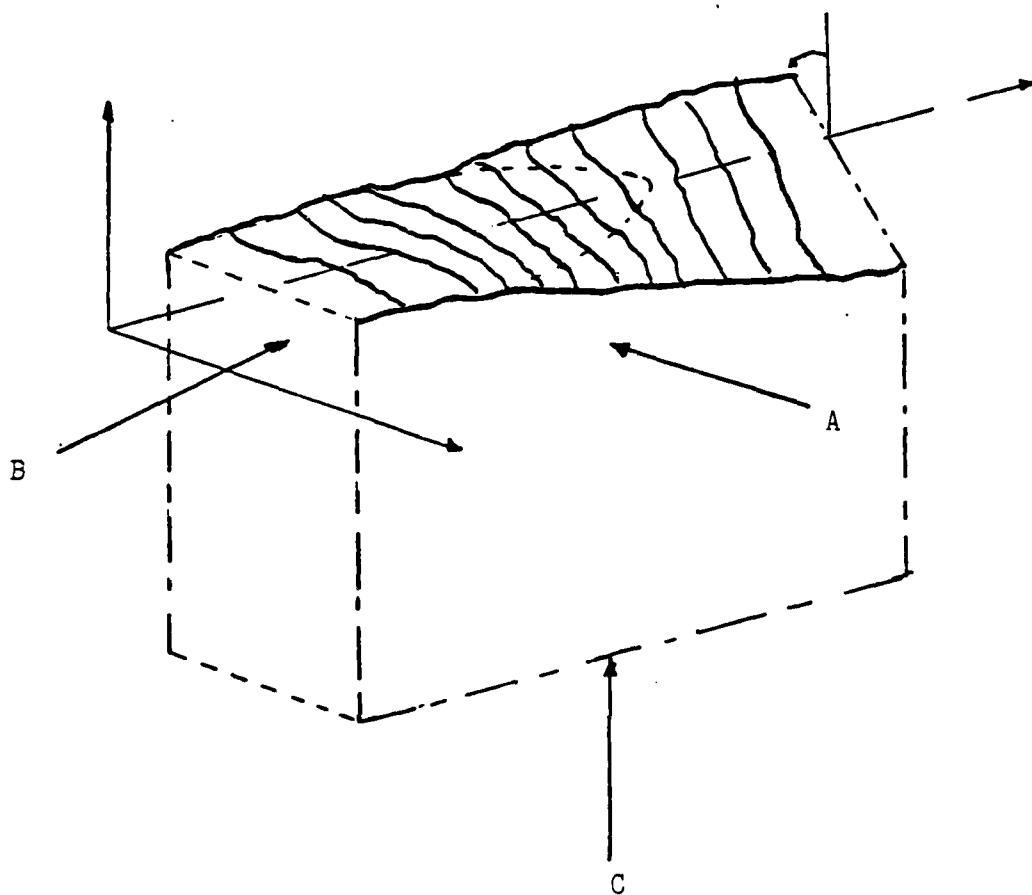


FIGURE 4.10 OPTICAL MICROGRAPH LOCATIONS FOR THE 9 AND 25 HOUR SOLUTION TREATED Mn CONTAINING ALLOYS, AND Cu CONTAINING ALLOYS.

FATIGUE CRACK PROPAGATION BEHAVIOR 303A

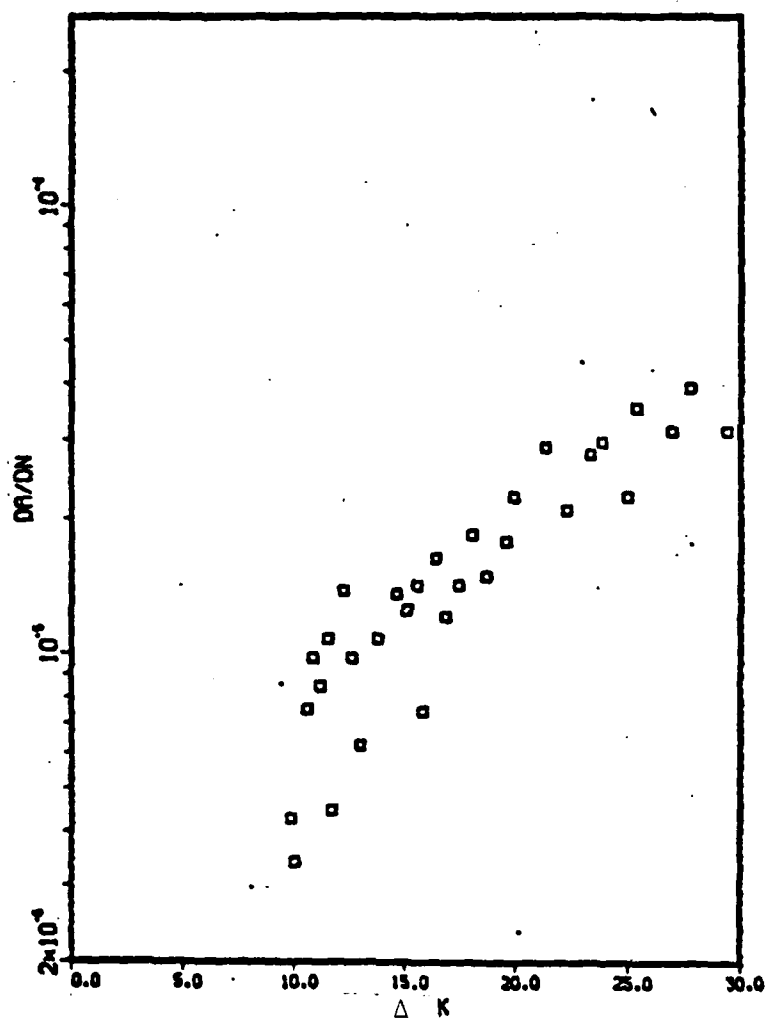


FIGURE 4.11 FATIGUE CRACK GROWTH DATA FOR Al-8.14 WT PCT  
Mg-0.40 WT PCT Cu ALLOY.



FIGURE 4.12 SCANNING ELECTRON FRACTOGRAPH FOR THE Al-8.14  
WT PCT Mg-0.40 WT PCT Cu ALLOY

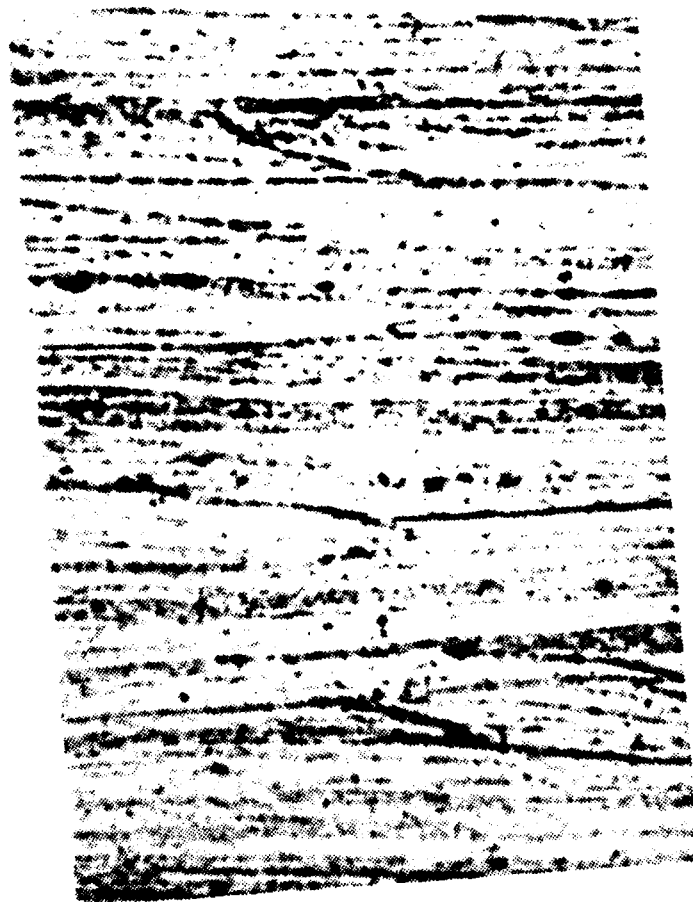


FIGURE 4.13 OPTICAL MICROGRAPH FOR THE Al-8.14 WT PCT  
Mg-0.40 WT PCT Cu ALLOY

## V. CONCLUSIONS AND RECOMMENDATIONS

### A. CONCLUSIONS

1. Crack growth measurements can be made in these alloys using equipment available.

2. Data aquisition/analysis methods used need to be improved to reduce scatter.

3. The crack growth characteristics determined for 7075-T6 are consistent with previous studies.

4. Al-10.2 wt pct Mg-0.52 wt pct Mn is a high strength alloy but exhibits poor crack growth characteristics. This can be attributed to the Mn Al<sub>6</sub> phase present in the alloy. The more Mn Al<sub>6</sub> formed and/or the coarser it is, the poorer the crack growth behavior.

5. The Al-8.14 wt pct Mg-0.40 wt pct Cu alloy exhibits a relatively high threshold  $\Delta k$  and generally better crack growth resistance than the 7075-T6. The alloy has a diffuse cell structure, relatively little precipitated beta and no constituent particles associated with cell or grain boundaries. All of these factors may contribute to this enhanced crack growth resistance.

### B. RECOMMENDATIONS

1. Extend these measurements to consider binary Al-Mg alloys, to eliminate third element effects.

2. Conduct further processing studies to control the amount and type of phases precipitated to evaluate the effects of these phases on crack growth.

3. Develop strength-toughness and strength-crack growth data to correlate with data available for existing alloys.

## FORTRAN PROGRAM FATIGUE 1

**25 FEB 83-2**

THIS PROGRAM IS DESIGNED TO PROVIDE ONE STEP DATA PROCESSING WHEN CONDUCTING RESEARCH IN THE AREA OF FATIGUE CRACK GROWTH RATE. THIS PROGRAM PROVIDES INPUT FOR FATIGUE2 FORTRAN.

\*NOTE\* IF YOU WANT A PLOT USE FATIGUE2 PROGRAM

P - LOAD (LBS)  
AM(1) - INITIAL CRACK LENGTH (IN)  
NR - NUMBER OF CYCLES  
AR - CRACK LENGTH RIGHT  
AL - CRACK LENGTH LEFT  
DELTA K - K  
DA/DN - INCHES/CYCLE  
W - WIDTH  
B - THICKNESS

```

INTEGER DATE, SAMPLE
DIMENSION AM(1000),OK(1000),OASN(1000),N(1000),AM2(1000)
N(1) = 0
PI= 3.14159
Q= 0.0835
W= 1.875

```

```

50 WRITE(5,50)
   FORMAT(5X,'[INPUT DATE: YR,MO,DA. ,SAMPLE NUMBER, ALLOY*)
   READ(5,5) DATE,SAMPLE,ALLOY
   WRITE(7,5) DATE, SAMPLE, ALLOY
   WRITE(5,51) DATE,SAMPLE,ALLOY
51 FORMAT(5X,'DATE ',18.5X,'SAMPLE NUMBER',15.5X,'ALLOY',F7.2,/)

```

```

100 WRITE(5,100)
   FORMAT(3X,' INPUT MAX LOAD:(LBS)'.3X,'MIN LOAD:(LBS)'.3X
   &,'INITIAL CRACK LENGTH (IN)')
   READ(5,&)PMAX,PMIN,AM(1)
   WRITE(7,&) PMAX, PMIN, AM(1)
   WRITE(6,101)PMAX,PMIN,AM(1)
101 FORMAT(1X,'MAX LOAD:'.F7.2,' LBS'.2X,'MIN LOAD:'.F7.2,' LBS'.2X
   &,'INIT CRACK LENGTH'.F6.5,' INCH'./)
   WRITE(5,110)
110 FORMAT(3X,'INPUT CRACK GROWTH RIGHT, CRACK GROWTH LEFT, # OF CYCLE
   &S')

```

```

111 WRITE(5,111)
    FORMAT(5X,'ENTER -100.0.0 TO EXIT')
112 WRITE(6,112)
    FORMAT(5X,'DELTA K (PSI/SQRT(IN))'.15X,'DA/DN (IN/CYCLE)'.//)
    DP = PMAX - PMIN
    DO 200 I=2,1000
        READ(5,*)AR,AL,N(I)
        WRITE(7,*) AR, AL, N(I)
        IF(AR.EQ.-100) GO TO 250
        AM2(I) = ((AM+AL)/32.0)+AM(I)
        AM(I) = AM2(I) / 2.0
        DK(I) = (DP/3)*SQRT((PI*(AM(I))/((W**2.0)*COS(PI*(AM(I)/W))))
        DADN(I) = (AM2(I)-AM2(I-1))/(FLOAT(N(I))-FLOAT(N(I-1)))
        IF(DADN(I-1).LT.0.0) DADN(I-1)=-1*DADN(I-1)
        WRITE(6,120)DK(I),DADN(I)
        FORMAT(10X,F12.3,23X,E15.5//)
120 CONTINUE
200 WRITE(7,260)
250 FORMAT(1X,'-100 0 0'.//)
60 STOP
END

```

# APPENDIX B

## FORTRAN PROGRAM FATIGUE 2

FILE: FATIGUE2 FORTRAN A1 NAVAL POSTGRADUATE SCHOOL

25 FEB 83-2

THIS PROGRAM IS DESIGNED TO PROVIDE ONE STEP DATA PROCESSING WHEN CONDUCTING RESEARCH IN THE AREA OF FATIGUE CRACK GROWTH RATE. ADDED TO THIS PROGRAM IS THE DISPLAY SUB-PROGRAM THAT WILL PLOT ALL DATA ON THE TEXTRONIX PRINTER.

P - LOAD (LBS)  
AM(1) - INITIAL CRACK LENGTH (IN)  
N - NUMBER OF CYCLES  
AR - CRACK LENGTH RIGHT  
AL - CRACK LENGTH LEFT  
DELTA K -  $\frac{K}{\Delta N}$   
DA/DN - INCHES/CYCLE  
W - WIDTH  
B - THICKNESS

INTEGER DATE, SAMPLE  
DIMENSION AM(1000), DK(1000), DADN(1000), N(1000), AK(1000), AM2(1000)  
N(1) = 0  
P = 3.14159  
B = 0.0935  
W = 1.475

READ(7,\*) DATE, SAMPLE, ALLOY  
WRITE(6,51) DATE, SAMPLE, ALLOY  
51 FORMAT(3X, 'DATE ', 18, 5X, 'SAMPLE NUMBER', 15, 5X, 'ALLOY ', F7.2, /)

READ(7,\*) PMAX, PMIN, AM(1)  
WRITE(6,101) PMAX, PMIN, AM(1)  
101 FORMAT(1X, 'MAX LOAD:', F7.2, ' LBS', 2X, 'MIN LOAD:', F7.2, ' LBS', 2X, 'INIT CRACK LENGTH', F6.5, ' INCH', //)

WRITE(6,112)  
112 FORMAT(5X, 'DELTA K (KSI/SQRT(IN))', 22X, 'DA/DN (IN/CYCLE)', //)

DP = PMAX - PMIN  
DO 200 I=2,1000  
150 READ(7,\*) AR, AL, N(I)  
IF(AR.EQ.-100) GO TO 250  
NPJINT = I-1  
AM2(I) = ((AR+AL)/32.0) + AM(1)  
AM(I) = AM2(I) / 2.0  
IF (AM(I)-AM(I-1).GE.0.01) GO TO 150  
AK(I) = (DP/3) \* (SQRT((P\*AM(I))/((W\*\*2.0)\*COS(P\*(AM(I)/W)))))  
DK(I-1) = AK(I)/1000.0  
DAN(I-1) = (AM2(I)-AM2(I-1))/(FLOAT(N(I))-FLOAT(N(I-1)))  
IF(DADN(I-1).LT.0.0) DADN(I-1) = -1.0\*DADN(I-1)  
C  
WRITE(6,120) DK(I-1), DADN(I-1)  
120 FORMAT(10X, F12.3, 23X, E15.5, /)

200 CONTINUE  
250 CONTINUE  
CALL TEK618  
CALL RESET('ALL')  
CALL NOBROR

```

CALL BLOWUP (1.5)
CALL PAGE (H.5.11.0)
CALL AREA2D (6.0.8.5)
CALL XNAME('DELTA K'.7)
CALL YNAME('DA/DN'.5)
CALL HEADIN('FATIGUE CRACK PROPAGATION BEHAVIOR 300A '.44.1.0.1)
CALL FRAME
C CALL GRAF(0.0.10..40...0000001.10.E-1..1)
C CALL XREVTK
C CALL YREVTK
CALL YLJG(0.0.5.0.2E-6.4)
C CALL XLGAXS(2E-6.3.6.'DA/DN'.-5.0..5.)
C CALL YGAXS(46..-9.0.1.0.5.'DELTA K'.-7.7..0.)
C CALL SMOOTH
CALL CURVE(DK.DADN.NPOINT.-1)
C CALL GRID (5.10)
CALL ENDPL(0)
CALL DONEPL
STOP
END

```

APPENDIX C

FORTRAN PROGRAM RESULTS

SAMPLE NUMBER 10

ALLOY 7075T6

MAX LOAD: 1200 LBS

MIN LOAD: 50 LBS

INIT CRACK LENGTH .50 IN

DELTA K KSI/IN

DA/DN (IN/CYCLE)

7.40	0.233
7.45	0.892
7.58	0.173
7.69	0.351
7.75	0.211
7.82	0.976
7.88	0.372
7.94	0.976
8.01	0.600
7.94	0.781
8.33	0.114
8.40	0.434
8.46	0.600
8.53	0.710
8.59	0.520
8.73	0.111
8.86	0.339
8.93	0.325
9.06	0.120
9.20	0.976
9.27	0.372
9.55	0.548
9.84	0.173
10.13	0.651
10.29	0.781
10.44	0.625
10.92	0.919
11.60	0.844
11.87	0.106
12.34	0.930
12.73	0.173
12.94	0.223
13.48	0.169
13.82	0.156
14.06	0.173
14.81	0.120
15.65	0.137
15.95	0.195
17.27	0.223
18.43	0.246
19.31	0.347
20.81	0.292
21.67	0.260

SAMPLE NUMBER 11

ALLOY 7075T6

MAX LOAD: 1200 LBS MIN LOAD: 50 LBS

INIT CRACK LENGTH .50 IN

DELTA K KSI/IN

DA/DN (IN/CYCLE)

7.30	0.273
7.55	0.651
7.73	0.156
7.80	0.360
8.06	0.946
8.23	0.253
8.32	0.643
8.38	0.710
8.64	0.120
8.84	0.260
9.05	0.868
9.18	0.976
9.39	0.101
9.46	0.781
9.60	0.104
9.68	0.976
9.97	0.223
10.04	0.411
10.19	0.976
10.58	0.205
10.74	0.679
11.18	0.168
11.23	0.585
11.40	0.142
11.58	0.104
11.75	0.173
12.31	0.126
12.71	0.183
13.02	0.101
13.57	0.244
14.27	0.146
15.62	0.200
16.23	0.148
16.89	0.240
17.61	0.183
18.40	0.312
19.27	0.208
20.24	0.781
24.81	0.437

SAMPLE NUMBER 14

ALLOY 7075T6

MAX LOAD: 1200 LBS

MIN LOAD: 50 LBS

INIT CRACK LENGTH .43 IN

DELTA K KSI/IN

DA/DN (IN/CYCLE)

6.62	0.261
6.68	0.831
6.81	0.622
7.00	0.275
7.06	0.169
7.25	0.339
7.44	0.442
7.50	0.789
7.75	0.332
7.88	0.274
8.14	0.568
8.20	0.130
8.33	0.390
8.59	0.428
8.73	0.236
8.86	0.312
8.98	0.370
9.19	0.756
9.55	0.625
9.69	0.504
9.91	0.868
9.98	0.300
10.13	0.318
10.29	0.173
10.60	0.946
10.92	0.306
11.25	0.504
11.77	0.689
12.05	0.901
12.24	0.625
12.73	0.930
13.37	0.600
13.59	0.710
13.94	0.349
14.55	0.156
15.08	0.260
15.65	0.801
16.10	0.633
16.92	0.162
17.27	0.558
18.43	0.260
19.54	0.488
20.54	0.588

SAMPLE NUMBER 15

ALLOY 7075T6

MAX LOAD: 1200 LBS

MIN LOAD: 50 LBS

INIT CRACK LENGTH .46 IN

DELTA K KSI/IN

DA/DN (IN/CYCLE)

6.74	0.939
6.81	0.507
6.93	0.157
7.12	0.106
7.50	0.978
7.63	0.190
7.82	0.119
7.94	0.146
8.14	0.217
8.33	0.478
8.53	0.183
8.79	0.372
9.41	0.558
9.69	0.240
9.98	0.164
10.29	0.381
10.60	0.488
10.84	0.710
10.92	0.372
11.25	0.148
11.96	0.932
12.73	0.718
13.04	0.101
13.37	0.137
13.77	0.200
13.94	0.377
14.30	0.868
14.55	0.781
14.95	0.180
15.36	0.213
15.95	0.111
16.58	0.208
17.27	0.120
18.03	0.156
18.64	0.101
20.28	0.248

SAMPLE NUMBER 5  
MAX LOAD: 1500 LBS

ALLOY 303A  
MIN LOAD: 50 LBS INIT CRACK LENGTH .48 IN

DELTA K KSI/IN

DA/DN (IN/CYCLE)

9.861	0.427
10.02	0.339
10.18	0.130
10.59	0.751
10.84	0.976
11.17	0.844
11.51	0.107
11.69	0.446
12.22	0.137
12.59	0.976
12.97	0.625
13.36	0.183
13.77	0.107
14.62	0.135
15.08	0.125
15.55	0.142
15.80	0.744
16.39	0.163
16.85	0.120
17.42	0.142
18.03	0.183
18.68	0.148
19.55	0.177
19.92	0.223
21.34	0.287
22.25	0.208
23.78	0.585
24.94	0.223
26.95	0.312
27.71	0.390
29.39	0.312

SAMPLE NUMBER 6  
MAX LOAD: 1150 LBS

MIN LOAD: 50 LBS

ALLOY 300A  
INIT CRACK LENGTH .48 IN

DELTA K KSI/IN

DA/DN (IN/CYCLE)

6.75	0.318
6.87	0.372
6.99	0.269
7.17	0.101
7.60	0.926
7.72	0.919
7.97	0.223
8.35	0.223
8.75	0.345
9.00	0.329
9.27	0.347
9.69	0.390
10.29	0.694
10.76	0.520
11.26	0.781
11.80	0.937
12.37	0.937
13.00	0.117

SAMPLE NUMBER 9  
MAX LOAD: 950 LBS

MIN LOAD: 50 LBS

ALLOY 300A  
INIT CRACK LENGTH .48 IN

DELTA K KSI/IN

DA/DN (IN/CYCLE)

5.62	0.621
5.82	0.130
6.02	0.156
6.32	0.468
6.42	0.488
6.52	0.625
6.72	0.120
6.93	0.260
7.04	0.315
7.25	0.168
7.36	0.142
7.47	0.223
7.73	0.189

## LIST OF REFERENCES

1. Shirah, R.H., The Influence of Solution Treatment Time and Quench Rate on Mechanical Properties of High Magnesium Aluminum Alloys, M.S. Thesis, Naval Postgraduate School, Monterey, California, December 1981.
2. Johnson, R.B., The Influence of Alloy Composition And Thermo-Mechanical Processing Procedure on Microstructure and Mechanical Properties of High-Magnesium Aluminum Magnesium Alloys, M.S. Thesis, Naval Postgraduate School, Monterey, California, June 1980.
3. Cadwell, C.A., Jr., Fatigue Characteristics and Micro-Structural Analysis of Thermomechanically Processed, High Magnesium Aluminum-Magnesium Alloy, M.S. Thesis, Naval Postgraduate School, Monterey, California, June 1981.
4. American Society for Testing Materials E647-81, Standard Test Method for Constant-Load Amplitude Fatigue Crack Growth Rates Above 10 m/cycle, ASTM, 1981.
5. American Society of Metals, Metals Handbook, Ninth Edition, Volume 2, Properties and Selection of Non Ferrous Alloys and Pure Metals, Page 44-62, American Society for Metals, 1979.
6. American Society of Metals, Metals Handbook, Ninth Edition, Volume 2, Properties and Selection of Non Ferrous Alloys and Pure Metals, Page 210, American Society for Metals, 1979.
7. Edwards, P.R., Method of Obtaining Crack Growth Data in Metals, Structures Department, Royal Aircraft Establishment, Farnbough, Hants., England October 1981.
8. American Society of Metals, Metals Handbook, Ninth Edition, Volume 2, Properties and Selection of Non Ferrous Alloys and Pure Metals, Page 142, American Society for Metals, 1979.
9. Hertzberg, R.W., Deformation and Fracture Mechanics of Engineering Materials, John Wiley and Sons, New York, New York, 1976.
10. Frost, N.E., Marsh, K.J., Pook, L.P., Metal Fatigue, Clarendon Press Oxford, England, 1974.

11. Garg, A., Naval Postgraduate School, Monterey, California,  
Unpublished Research, 1983.

# INITIAL DISTRIBUTION LIST

	No. Copies
1. Defense Technical Information Center Cameron Station Alexandria, Virginia 22314	2
2. Library, Code 0142 Naval Postgraduate School Monterey, California 93940	2
3. Department Chairman, Code 69Mx Department of Mechanical Engineering Naval Postgraduate School Monterey, California 93940	1
4. Professor T.R. McNelley, Code 69Mc Department of Mechanical Engineering Naval Postgraduate School Monterey, California 93940	5
5. Mr. Richard Schmidt, Code AIR 320A Naval Air Systems Command Naval Air Systems Command Headquarters Washington, DC 20361	1
6. Adjunct Professor D.E. Peacock, Code 69P Department of Mechanical Engineering Naval Postgraduate School Monterey, California 93940	1
7. LT Kurt D. Oberhofer USN SWOSCOLCOM Naval Station Newport, RI 02840	3

